Hindawi
International Transactions on Electrical Energy Systems
Volume 2022, Article ID 7827164, 21 pages
https://doi.org/10.1155/2022/7827164

Research Article

An Improved Equilibrium Optimizer Algorithm for Solving Optimal Power Flow Problem with Penetration of Wind and Solar Energy

Ngoc Anh Nguyen,[1,2] **Dieu Ngoc Vo**,[1,3] **Thuan Thanh Nguyen**,[2] **and Thanh Long Duong**[2]

[1]*Department of Power Systems, Ho Chi Minh City University of Technology (HCMUT), 268 Ly Thuong Kiet Street, District 10, Ho Chi Minh City, Vietnam*
[2]*Faculty of Electrical Engineering Technology, Industrial University of Ho Chi Minh City, Ho Chi Minh City, Vietnam*
[3]*Vietnam National University Ho Chi Minh City, Linh Trung Ward, Thu Duc, Ho Chi Minh City, Vietnam*

Correspondence should be addressed to Thanh Long Duong; duongthanhlong@iuh.edu.vn

Received 2 January 2022; Revised 30 April 2022; Accepted 10 May 2022; Published 30 June 2022

Academic Editor: Tianqi Hong

The paper is proposed an improved equilibrium optimizer (IEO) algorithm to solve the optimal power flow (OPF) problem with the participation of a renewable energy source (RES). In the proposed IEO method, the "exponential term" is replaced by a function that does not dependent on the number of iterations. This modification of the IEO algorithm increases exploration ability compared to EO algorithm. In addition, the exploration of the proposed IEO algorithm will not decrease according to the number of iterations which avoids to get stuck at the local optimal solution. The IEO algorithm is tested on two IEEE 30-bus and IEEE 118-bus systems with three different objective functions. The performance of the proposed IEO method is compared with equilibrium optimizer (EO), artificial ecosystem optimization (AEO), cuckoo search algorithm (CSA), teaching-learning-based optimization (TLBO), artificial bee colony (ABC), and many other existing methods. Besides, a simple probabilistic formula for calculating RES output power based on the Monte-Carlo simulation model is proposed in this paper to reduce the computation time for the OPF problem with RES. The simulation results obtained show that the proposed IEO algorithm has better quality of the solution as well as stability level compared to the original EO algorithm and other algorithm. Thus, the proposed IEO algorithm is also one of effective and reliable algorithms for handling OPF problem with RES.

1. Introduction

Optimal power flow (OPF) is an optimizing tool for power system planning and operation. The OPF has been received significant interest of power system optimization research group since first introduced in 1962 [1]. The main aim of the OPF problem is to determine the optimal setting control variables which optimize chosen objective functions such as fuel cost, emission cost, power loss, and voltage profile while satisfying a set of operational and physical constraints. The control variables of the OPF problem are that the actual power at the generator buses, excluding the slack bus, the voltage magnitude at all the generator buses, tap changer of transformer, and shunt compensators. Many mathematical programming methods have been deployed to deal with OPF problems, such as linear programming (LP) [2], nonlinear programming (NLP) [3], Newton-based techniques [4], quadratic programming (QP) [5], and interior-point (IP) methods [6]. However, the objective functions of the OPF problem, which was solved by these conventional methods, are simple and differentiable. In addition, the energy sources of the conventional OPF problem only involved thermal power sources. In fact, the OPF problem in modern power systems is always a nonlinear optimization problem and may

be a nondifferentiable one; thus, it is an actual challenge for optimization methods for dealing with, especially, the conventional methods. In order to overcome the limitations of classical methods, heuristic methods have been considered as alternative approaches to solve the OPF problem with the advantages of obtaining nearly optimum solution whether the problem is differentiable or not.

In recent decades, heuristic optimization algorithms have been developed based on inspired from physical phenomena, animal behavior, or evolutionary concepts. They provide straightforward and effective solutions for the OPF problem. The typical algorithms such as particle swarm optimization (PSO) [7], gravitational search algorithm (GSA) [8, 9], differential evolutionary (DE) [10], krill herd algorithm (KHA) [11], artificial bee colony (ABC) [12], biogeography-based optimization (BBO) [13], Jaya algorithm [14], harmony search (HS) [15], teaching-learning-based-optimization technique (TLBO) [16], Sine-Cosine (SC) [17], grey wolf optimizer (GWO) [18], and moth swarm approach (MSA) [19]. The objective functions of the OPF problem usually are considered consisting of three different types of fuel functions, namely, quadratic cost, piecewise quadratic cost, quadratic cost curve, and power loss, emission cost and voltage deviation. In addition, the objective of maximum social welfare [20] and available transfer capability [21] are also used when solving the OPF problem by heuristic optimization algorithms. In general, these methods are successfully applied in the OPF problem. However, the solution of these algorithms often falls into the local optimum for the large-scale power system.

So, in order to improve the solution quality and efficiency of the metaheuristic methods, the hybrid and improved algorithms have been proposed to solve the OPF problem [22–30]. The goal of the hybrid algorithms is to achieve optimal balance between exploration and exploitation strategy. In [22], a hybrid (SFLA-SA) algorithm of simulated annealing algorithms (SFLAs) with the probabilistic shuffle jump characteristic of the shuffled frog algorithm (SA) is proposed to avoid stagnation at the local solution of SFLA. In [23], the hybrid (PSO-GSA) algorithm is proposed for the OPF problem by combining the social thinking ability in PSO and the local search ability of GSA to reach the better solution quality compared to PSO. In [24], the hybrid algorithm between cuckoo search algorithm (CSA) and sunflower algorithm (SFO) (HCSA-SFO) is proposed, wherein the Lévy flight function of CSA has been replaced by the mutation and selection mechanism of SFO to reach the higher solution quality and shorter executed time over CSA. Many studies have been proposed in recent years with aims of improving exploration performance or the solution quality by using random jumps of Lévy flight or mutation vector to increase diversity of population such as the improved grey wolf optimizer (DGWO) [25], modified honey bee mating optimization (MHBMO) [26], and skip shuffle modification (MSFL) [27]. An improved moth-flame optimization algorithm (IMFA) for solving optimal power flow problem is proposed in [28]. In [29], the improved collision object optimization (ICBO) algorithm is proposed by using three colliding objects instead of two objects collision as the original algorithm. A modified imperialist competitive algorithm (MICA) with a review of the imperial power mechanism to promote global optimization has been proposed in [30] to improve the simulation time as well as the optimal solution. These hybrid or improved algorithms in general have yielded significant performance compared to the original version in terms of obtained solution quality as solving the OPF problems which have many local optimizations.

Nowadays, renewable energy sources (RESs) including wind power and solar energy are gradually replacing conventional thermal power plants due to advantages of these energy sources. Integrating wind and solar power on the traditional grid can have significant impact on the efficiency of power system operation. However, they have posed many difficulties in planning and operating the power system due to their uncertain and discontinuous nature. Therefore, solving the optimal power system (OPF) problem to minimize the objective functions in the power system containing traditional power plants and renewable energy power plants is one of the important tasks for the independent operator system.

Several published papers related to the OPF problem in the power system including conventional power plants and renewable energy power plants have been presented in recent years. Optimization methods are widely used to solve problems related to penetration of renewable energy. A hybrid Harris hawks optimizer for integration of renewable energy sources considering stochastic behavior of energy sources is proposed in [31]. In [32], authors have been proposed differential evolutionary particle swarm optimization to deal with optimal power flow of power systems with controllable wind-photovoltaic energy systems. A barnacle mating optimizer (BMO) has been proposed to solve the optimal power flow (OPF) problem with and without renewable energy sources [33]. The effectiveness of the proposed BMO in solving the OPF is tested on a modified IEEE-30 bus system that is integrated with solar PV farms. In [34], authors have been proposed an algorithm hybrid based on combination of phasor particle swarm optimization and a gravitational search algorithm (PPSOGSA) for the OPF in power systems with an integrated wind turbine (WT) and solar photovoltaic (PV) generators. The forecasted active power of WT and PV are considered as dependent variables in the OPF formulation, while the voltage magnitude at WT and PV buses is considered as control variables. Forecasting the output power of WT and PV generators is based on the real-time measurements and the probabilistic models of wind speed and solar irradiance. In [35], the authors have been used the genetic algorithm (GA) and the two-point estimation method to solve the OPF problem integrating wind and solar energy. A hybrid method of moth swarm algorithm and gravitational search algorithm (HMSAGSA) is used to solve OPF problems including wind energy [36]. The improved two-point estimation method is proposed to solve the OPF problem combining wind and photovoltaic cells [37]. A self-adaptive evolutionary programming (SAEP) [38] is applied to solve OPF with combined wind energy. A number of

other algorithms are proposed to solve OPF problems with integrated renewable energy sources as introduced in [39–46]. In general, these methods are applied in the OPF problem with RES. However, the simulation results only are tested on IEEE 30 bus system with RES while the IEEE 118 bus system is tested without RES.

Recently, an algorithm equilibrium optimizer (EO) is developed by Faramarzi et al. [47]. The EO has fast convergence ability, but it is also easy to fall in local minima. In order to overcome the limit, this paper is proposed an improved equilibrium optimizer algorithm (IEO) for solving the OPF problem with integrated renewable energy sources. In the IEO, the exponential term is replaced by a function that does not dependent on the number of iterations. This modification of the IEO algorithm increases exploration ability compared to the EO algorithm. In addition, the exploration of the IEO algorithm will not decrease according to the number of iterations that avoid to get stuck at the local optimal solution. The proposed IEO method is tested on the modified IEEE 30-bus and 118-bus systems with RESs, and simulation results are compared with many other methods. The simulation results obtained show that the proposed IEO algorithm provides quality solution and stability ability with other objective functions. Thus, the proposed method is an alternative approach quite promising for solving optimal power flow problems. The main contributions in this paper are as follows:

- A new improved IEO algorithm for solving OPF problem with RES, which improves quality solution and stability level, is proposed in this paper.
- A simple probabilistic formula for calculating RES output power based on the Monte-Carlo simulation model is proposed to reduce the computation time for the OPF with RES.
- A modified IEEE 118-bus system with wind and solar power plants is introduced in this paper.

The remaining organization of the paper is done as follows. Section 2 includes the mathematical model related to the OPF problem. In Section 3, uncertainty modelling of wind and solar power outputs is presented. Section 4 describes EO and IEO algorithms and the application of the IEO algorithm for the OPF problem. Section 5 gives simulation results. Finally, the conclusion is given in Section 6.

2. Problem Formulation

The two IEEE 30-bus and IEEE 118-bus systems integrating of wind and solar energy are considered in this study. The wind and solar power output are scheduled as like other fossil energy sources. However, the uncertainty of the RES output should require a combination of all generator outputs and reserve outputs for the system to operate in a balanced manner under all circumstances. Therefore, the total cost of generation includes fuel costs for fossil fuel generators, direct costs that ISO buys electricity from RES suppliers, penalty costs, and reserve costs. The generation cost models are described in the following sections.

2.1. Cost of Wind and Solar Photovoltaic Power. Wind or solar energy is a random quantity. Therefore, it is difficult to establish an accurate cost model for these energy sources. The authors in [41] have been introduced a model of costs for RES energy sources which is owned by ISO, no fuel costs. However, the excess or lack of this energy at a time is related to the overall operation cost of the power system. Thus, the correctly assessment of the scheduled capacity compared to the actual capacity of the RES sources will reduce the operation costs of the power system. There are two cases when constructing of the cost function for the RES sources. The actual capacity of the RES is less than the scheduled capacity, and the independent system operator (ISO) must dispatch power from other plants to make up for the shortfall of these sources. The cost of committing the reserve generating plants to meet over estimated amount is termed as reserve cost. Opposite, the scheduled capacity is less than the actual power of the RES, and the surplus power of RES will be wasted. This case needs to reduce power output from conventional generators if not possible to utilize RES. The ISO is required to pay a penalty cost corresponding to the surplus amount of RES. The steps to calculate the production cost of RES are described as shown in Figure 1.

2.1.1. Direct Cost of Wind and Solar Photovoltaic Power. Normally, wind or solar farms are owned by private operators. Therefore, the grid operator ISO incurs the cost of scheduled purchases of electricity from these private operators, and this cost is treated as a direct cost.

The direct cost of the j^{th} wind power plant in terms of scheduled power is modelled as follows:

$$C_{w,j}\left(P_{\text{s.wind},j}\right) = g_j P_{\text{s.wind},j}, \tag{1}$$

where g_j is coefficient of direct cost and $P_{\text{s.wind},j}$ is scheduled power of the j^{th} wind power plant.

The direct cost of the k^{th} solar power plant in terms of scheduled power is modelled as follows:

$$C_{s,k}\left(P_{\text{s.solar},k}\right) = h_k P_{\text{s.solar},k}, \tag{2}$$

where h_k is the direct cost coefficient and $P_{\text{s.solar},k}$ is the scheduled power of the k^{th} solar power plant.

2.1.2. Penalty Costs of Wind and Solar Plants. The overestimation of RES occurs when the actual power output is lower than the scheduled power output. Therefore, ISO needs to mobilize from other energy sources and additional costs are incurred. The incurred costs for this mobilization are shown as follows:

Reserve cost for the j^{th} wind plant is

$$\begin{aligned} C_{wL,j} = & K_{wL,j} \cdot f_{w,j}\left(P_{\text{wind},j} < P_{\text{s.wind},j}\right) \\ & \cdot \left(P_{\text{s.wind},j} - E_{P_{\text{wind},j} < P_{\text{s.wind},j}}\left(P_{\text{wind},j}\right)\right), \end{aligned} \tag{3}$$

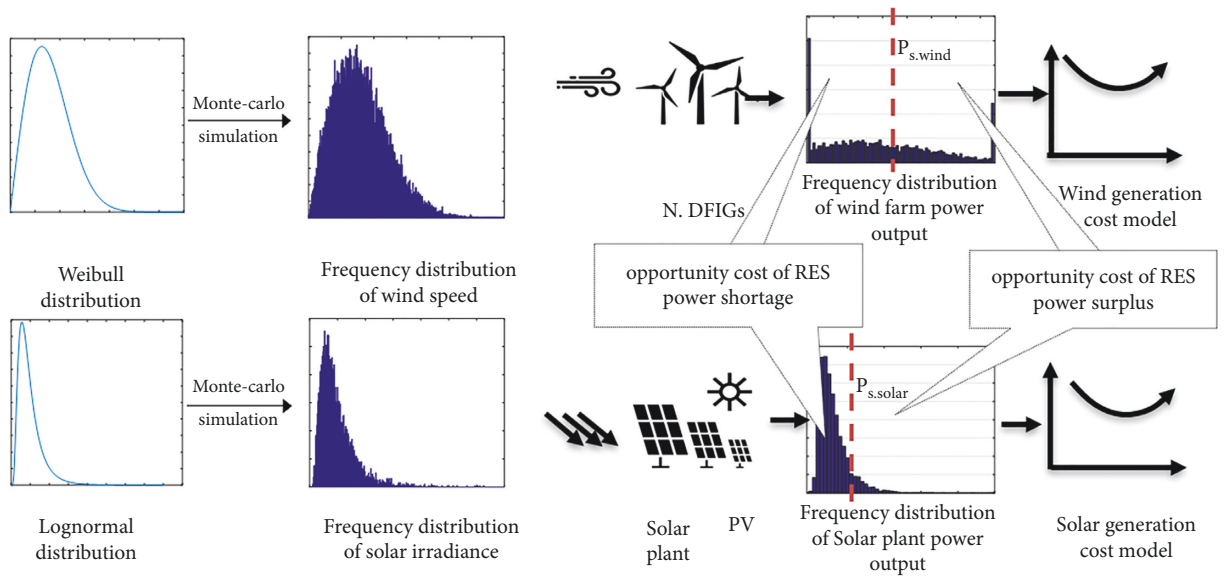

Figure 1: Cost calculation model for RES source.

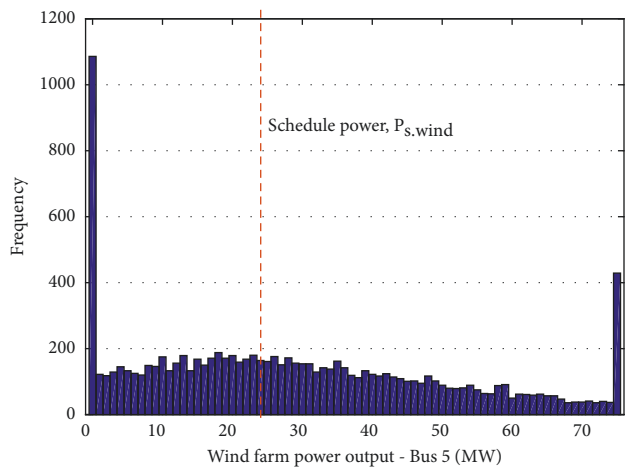

Figure 2: Wind power distribution for wind farm #1 at bus 5 (C = 9, k = 2).

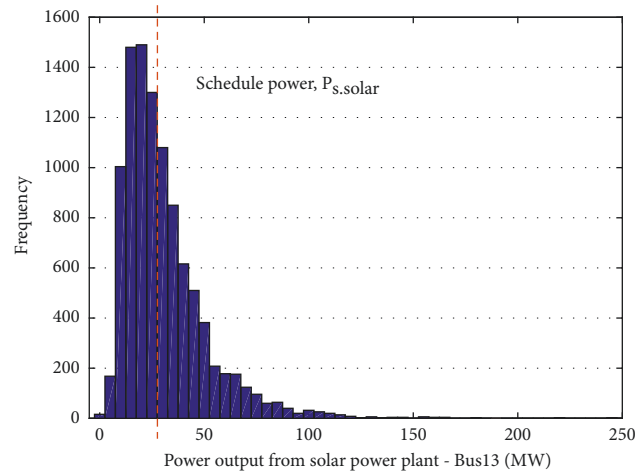

Figure 3: Power output distribution from solar power plant at bus 13 ($\mu = 6$, $\sigma = 0.6$).

where $C_{wL,j}$ is the incurred cost for the shortfall of wind power output, $P_{\text{wind},j}$ is the actual capacity of the wind farm that is less than the scheduled capacity$P_{\text{s.wind},j}$, $f_{w,j}(P_{\text{wind},j} < P_{\text{s.wind},j})$ is probability of wind power shortage, $E_{P_{\text{wind},j} < P_{\text{s.wind},j}}(P_{\text{wind},j})$ is the scheduled wind power output according to $P_{\text{wind},j} < P_{\text{s.wind},j}$, the scheduled value of the left half-plane in Figure 2, and $K_{wL,j}$ is the coefficient of the incurred cost.

Reserve cost for the k^{th} solar plant is

$$C_{sL,k} = K_{sL,k} \cdot f_{s,k}\left(P_{\text{solar},k} < P_{\text{s.solar},k}\right) \cdot \left(P_{\text{s.solar},k} - E_{P_{\text{solar},k} < P_{\text{s.solar},k}}\left(P_{\text{solar},k}\right)\right), \quad (4)$$

where $C_{sL,k}$ is the incurred cost for the shortfall of solar power $P_{\text{s.solar},k}$, $P_{\text{solar},k}$ is the scheduled and actual solar power output, $f_{s,k}(P_{\text{solar},k} < P_{\text{s.solar},k})$ is the probability of a solar power shortage$E_{P_{\text{solar},k} < P_{\text{s.solar},k}}(P_{\text{solar},k})$ is the scheduled power output of solar below $P_{\text{solar},k} < P_{\text{s.solar},k}$, the scheduled value of the left half-plane in Figure 3, and $K_{sL,k}$ is the coefficient of the incurred costs.

2.1.3. Opportunity Cost of Wind and Solar Power Surplus. Similarly, the underestimation of RES occurs when the actual energy is higher than the estimated value. As a result, ISO incurs a penalty fee. This cost can be expressed as follows:

Penalty cost for the underestimation of j^{th} wind plant is

$$C_{wH,j} = K_{wH,j} \cdot f_{w,j}\left(P_{\text{wind},j} > P_{\text{s.wind},j}\right) \cdot \left(E_{P_{\text{wind},j} > P_{\text{s.wind},j}}\left(P_{\text{wind},j}\right) - P_{\text{s.wind},j}\right), \tag{5}$$

where $C_{wH,j}$ is the penalty cost of wind power surplus, $f_{w,j}(P_{\text{wind},j} > P_{\text{s.wind},j})$ is the probability of a wind power surplus, $E_{P_{\text{wind},j} > P_{\text{s.wind},j}}(P_{\text{wind},j})$ is the scheduled of power wind output under $P_{\text{wind},j} > P_{\text{s.wind},j}$, the scheduled value of right half-plane in Figure 2 (in kW), and $K_{wH,j}$ is penalty cost of wind power surplus.

Penalty cost for the underestimation of k^{th} solar plant is

$$C_{sH,k} = K_{sH,k} \cdot f_{s,k}\left(P_{\text{solar},k} > P_{\text{s.solar},k}\right) \cdot \left(E_{P_{\text{solar},k} > P_{\text{s.solar},k}}\left(P_{\text{solar},k}\right) - P_{\text{s.solar},k}\right), \tag{6}$$

where $C_{sH,k}$ is the penalty cost of the solar surplus, $f_{s,k}(P_{\text{solar},k} > P_{\text{s.solar},k})$ is the probability of a solar surplus; $E_{P_{\text{solar},k} > P_{\text{s.solar},k}}(P_{\text{solar},k})$ is the scheduled of solar power output under $P_{\text{solar},k} > P_{\text{s.solar},k}$, the scheduled value of right half-plane in Figure 3 (in kW), and $K_{sH,k}$ is penalty cost of solar surplus.

The total cost of wind power generated from a wind farm and solar power is described as follows:

$$C_{\text{wind}} = \sum_{j=1}^{N_{\text{wind}}} \left(C_{w,j}\left(P_{ws,j}\right) + C_{wL,j} + C_{wH,j}\right),$$
$$C_{\text{solar}} = \sum_{k=1}^{N_{\text{solar}}} \left(C_{s,k}\left(P_{ss,k}\right) + C_{sL,k} + C_{sH,k}\right). \tag{7}$$

2.2. Objective Function. In the study, three different objective functions including generation cost, total emission, and power losses are considered in the OPF problem integrating wind and solar power on the traditional grid.

2.2.1. Generation Cost.

$$FC = F_C + C_{\text{wind}} + C_{\text{solar}}. \tag{8}$$

where F_C is cost function of thermal power generators. $C_{\text{wind}}, C_{\text{solar}}$ are the costs of wind and solar energy, respectively.

Fuel costs for thermal power plants using fossil fuels can be approximated according to the quadratic function as follows:

$$F_C = \sum_{i=1}^{N_{TG}} \left(a_i + b_i P_{TGi} + c_i P_{TGi}^2\right) \cdot \left(\frac{\$}{h}\right). \tag{9}$$

In fact, thermal power generators with multivalve steam turbines exhibit a greater variation in the fuel-cost functions. Therefore, the valve-point effect in terms of absolute value of the sinusoidal function needs to be considered in formula (9):

$$F_C = \sum_{i=1}^{N_{TG}} a_i + b_i P_{TGi} + c_i P_{TGi}^2 + \left|d_i + \sin\left(e_i \cdot \left(P_{TGi}^{\min} - P_{TGi}\right)\right)\right| \cdot \left(\frac{\$}{h}\right), \tag{10}$$

where a_i, b_i, c_i, d_i, and e_i are fuel cost coefficients of the i^{th} generator, while N_{TG} represents the total number of thermal power plants.

2.2.2. Total Emission. The total emissions *FE (ton/h)* of thermal power plants are given by

$$FE = \sum_{i=1}^{N_{TG}} \left(\alpha_i + \beta_i P_{TGi} + \gamma_i P_{TGi}^2\right) + \xi_i \exp\left(\lambda_i P_{TGi}\right) \cdot \left(\frac{\text{ton}}{h}\right), \tag{11}$$

where α_i, β_i, γ_i, ξ_i, and λ_i are emission factors of i^{th} thermal power plant.

2.2.3. Total Transmission Loss. The total power loss P_{loss} in the transmission network can be calculated according to the following formula:

$$P_{\text{loss}} = \sum_{i=1}^{N_G} P_{Gi} - \sum_{j=1}^{N_L} P_{Lj}\,(MW). \tag{12}$$

2.3. Constraints

2.3.1. Equality Constraints. Constraints on real and reactive power balance:

$$P_{Gi} - P_{Li} = |V_i| \sum_{j=1}^{N_B} |Y_{ij}||V_j| \cos\left(\delta_i - \delta_j - \theta_{ij}\right),$$
$$Q_{Gi} - Q_{Li} = |V_i| \sum_{j=1}^{N_B} |Y_{ij}||V_j| \sin\left(\delta_i - \delta_j - \theta_{ij}\right). \tag{13}$$

2.3.2. Inequality Constraints. The limits of power generation:

$$P_{Gi,\min} \le P_{Gi} \le P_{Gi,\max}, \quad i = 1, 2, \ldots, N_G, \tag{14}$$

$$Q_{Gi,\min} \le Q_{Gi} \le Q_{Gi,\max}, \quad i = 1, 2, \ldots, N_G. \tag{15}$$

The limits of generator voltage bus and load voltage bus:

$$V_{Gi,\min} \le V_{Gi} \le V_{Gi,\max}, \quad i = 1, 2, \ldots, N_G, \tag{16}$$

$$V_{Lj,\min} \le V_{Lj} \le V_{Lj,\max}, \quad j = 1, 2, \ldots, N_L. \tag{17}$$

The limits of transmission line:

$$S_l \le S_{l,\max}, \quad l = 1, 2, \ldots, N_{\text{Line}}. \tag{18}$$

The limits of switchable capacitor capacity:

$$Q_{ci,\min} \le Q_{ci} \le Q_{ci,\max}, \quad i = 1, 2, \ldots, N_C. \tag{19}$$

The limits of transformer tap:

$$T_{k,\min} \le T_k \le T_{k,\max}, \quad k = 1, 2, \ldots, N_T. \tag{20}$$

3. Uncertainty and Power Model of Wind and Solar PV Power Plants

3.1. Uncertainty and Power Model of Wind Power Plants. Unlike conventional thermal power generators, the characteristic of the output power generated by the wind turbine is a random variable depending on wind speed. The wind speed distribution follows the Weibull probability density function with a scale factor (C) and a shape factor (k). The probability of wind speed v (m/s) is given by

$$f_v(v) = \left(\frac{k}{C}\right)\left(\frac{v}{C}\right)^{(k-1)} e^{-(v/C)^k} \quad \text{for } 0 \le v < +\infty. \tag{21}$$

The average wind speed is determined by

$$\text{Mean}(v) = C \cdot \Gamma\left(1 + k^{-1}\right), \tag{22}$$

where $\Gamma(x)$ is gamma function and is described as follows:

$$\Gamma(x) = \int_0^\infty e^{-t} t^{x-1} \mathrm{d}t. \tag{23}$$

Wind speed following the Weibull distribution can be calculated as follows:

$$v = C \cdot (-\ln(r))^{1/k}, \tag{24}$$

where r is a random number uniformly distributed in the range [0,1].

Figures 4 and 5 show the best fit of the Weibull distribution and the frequency of wind output at bus 5 and bus 11 using 10000 Monte-Carlo scenarios, respectively. In the study, the value of the shape parameter (k) and scale parameter (C) for the simulation of wind farms is chosen as reference [41]. For the modified IEEE-30 bus system, $C = 9$ and $C = 10$ are assumed for two wind farms located at bus 5 and bus 11. The average wind speed of the two farms is 7,976 (m/s) and 8,862 (m/s), respectively, which is completely consistent with the design standards for wind turbine installations specified in [48], when the maximum allowable average wind speed is 10 m/s.

Relationship between power output of wind turbine and wind speed (v) is described as

$$P_{\text{wind}}(v) = \begin{cases} 0, & \text{for } v < v_{\text{in}} \text{ and } v > v_{\text{out}}, \\ P_{wr}\left(\dfrac{v - v_{\text{in}}}{v_r - v_{\text{in}}}\right), & \text{for } v_{\text{in}} < v < v_r, \\ P_{wr}, & \text{for } v_r < v < v_{\text{out}}, \end{cases} \tag{25}$$

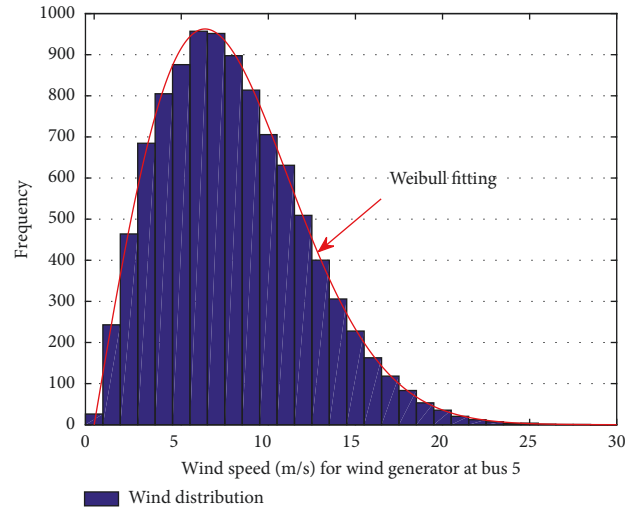

Figure 4: Wind speed distribution for wind farm #1 at bus 5 ($C = 9$, $k = 2$).

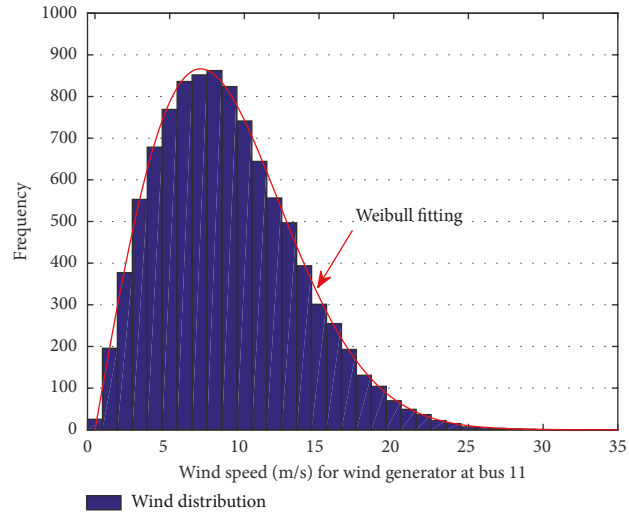

Figure 5: Wind speed distribution for wind farm #2 at bus 11 ($C = 10$, $k = 2$).

where v_{in}, v_{out}, and v_r are the cut-in wind speed, cut-out wind speed, and rated wind speed of the turbine, respectively. The rated output power of the wind turbine is P_{wr}.

According to formula (25) and the frequency distribution of wind speed, the distribution of power output of the wind farm at bus 5 can be described by the frequency distribution graph as shown in Figure 2. The dotted line shows the scheduled output power needed to supply to the grid.

3.2. Uncertainty and Power Model of Solar PV Power Plants. Similarly, the power model of wind plants, the random nature of solar radiation (H) is modelled according to a log-normal distribution function. The solar irradiance probability depends on the standard deviation (μ) and the mean (σ) as follows:

$$f_H(H) = \frac{1}{H\sigma\sqrt{2\pi}} e^{-\left((\log(H)-\mu)^2/2\sigma^2\right)}. \quad (26)$$

The average solar irradiance is determined by

$$\text{Mean}(H) = e^{\left(\mu+\left(\sigma^2/2\right)\right)}. \quad (27)$$

Figure 6 shows the fit between the log-normal distribution curve and the solar radiation frequency using 10000 Monte-Carlo scenarios. The solar irradiance (H) to energy conversion for solar PV is given by

$$\mathbf{P_{solar}}(\mathbf{H}) = \begin{cases} \mathbf{P_{sr}}\left(\dfrac{\mathbf{H}^2}{\mathbf{H_{std}R_c}}\right), & \textbf{for } 0 < \mathbf{H} < \mathbf{R_c}, \\ \mathbf{P_{sr}}\left(\dfrac{\mathbf{H}}{\mathbf{H_{std}}}\right), & \textbf{for } \mathbf{H} \geq \mathbf{R_c}, \end{cases} \quad (28)$$

where H_{std} is the solar irradiance in standard environment, R_c is a certain irradiance point, and P_{sr} is the rated output power of the solar PV unit. In this study, H_{std} and R_c are set to 800 (W/m^2) and 120 (W/m^2), respectively [41].

Similar to the wind farm, the distribution of power output from the solar power plant at bus 13 can be depicted by a histogram as shown in Figure 3.

3.3. Conditional Probabilities of Wind and Solar Energy Sources. In this paper, the calculation probability of wind power is proposed as equation (29). Based on the number of RES output power samples obtained from Monte-Carlo simulation, we can calculate the probability of the RES output power when the RES output power is smaller or larger than the scheduled capacity. The probability of RES output power is described as follows:

$$f_x(A < K \text{ or } A > K) = \frac{\sum P_{(A<K \text{ of } A>K)}}{N_{\text{Montecarlo}}}, \quad (29)$$

where X set is the output power of the RES determined through Monte-Carlo simulation, K is the scheduled power obtained from the algorithm's solutions, $f_x(A < K \text{ of } A > K)$ is the probability that the RES power is less than or greater than the scheduled power value K, and $N_{\text{Montecarlo}}$ is the number of Monte-Carlo samples.

4. Proposed Optimization Algorithm

4.1. Equilibrium Optimizer Algorithm. The equilibrium optimizer (EO) algorithm [47] is based on determining the dynamic equilibrium for the mass equilibrium model. The mathematical formula is described as follows:

$$\mathbf{G}\frac{\mathbf{dX}}{\mathbf{dt}} = \mathbf{QX_{eq}} - \mathbf{QX} + \mathbf{P}, \quad (30)$$

where matter concentration (X) represents the optimized search space. In the EO algorithm, the new particle concentration is updated based on the equilibrium concentration group X_{eq}, the exponential E, and the rate of generation P. The four main stages of EO can be summarized as follows.

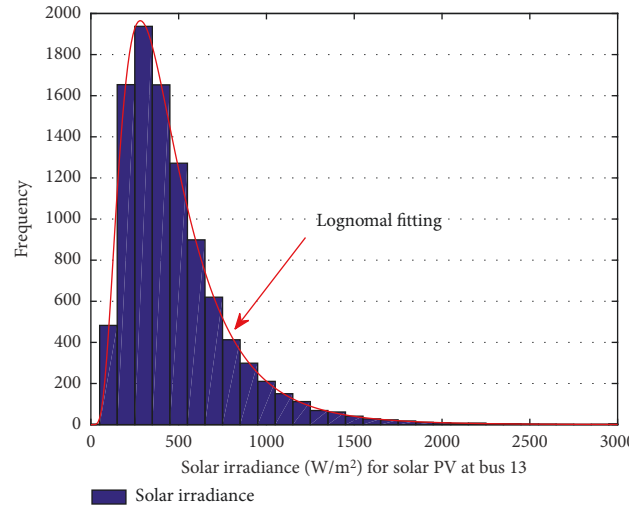

Figure 6: Solar irradiance distribution from solar power plant at bus 13 ($\mu = 6$, $\sigma = 0.6$).

4.1.1. Initialization. In this stage, the concentration of a particle is randomly initialized for the D-dimensional problem and the number of N_{pop} samples as follows:

$$\mathbf{X_{i,j}} = \mathbf{rand}[0, 1] \cdot \left(\mathbf{X_{max,j}} - \mathbf{X_{min,j}}\right) + \mathbf{X_{min,j}}, \quad (31)$$

where $i\varepsilon\{1, 2, \ldots, N_{\text{pop}}\}$, $j\varepsilon\{1, 2, \ldots, \text{Dim}\}$ and rand [0, 1] is a random number between 0 and 1.

4.1.2. Determine the Equilibrium Group. The four candidates in the $X_{\text{eq},i}$ equilibrium are considered to contribute to a better EO for exploration, while the average is for mining. The candidates at equilibrium including the four best solutions in the current population are represented in the following equation:

$$X_{\text{pool}} = \{X_{eq1}, X_{eq2}, X_{eq3}, X_{eq4}, X_{\text{avg}}\}, \quad (32)$$

where X_{eq1}, X_{eq2}, X_{eq3}, X_{eq4} is the best, second best, third best, and fourth best solution in the population; X_{avg} is the average candidate (average solution) of the four best individuals and obtained by the following equation:

$$\mathbf{X_{avg}} = \frac{\mathbf{X_{eq1}} + \mathbf{X_{eq2}} + \mathbf{X_{eq3}} + \mathbf{X_{eq4}}}{4}. \quad (33)$$

4.1.3. Exponential Term (E). The exponential term (E) is one of several that changes over time that will help EO strike the right balance between exploration and exploitation:

$$E = \alpha_1 \text{sign}(r - 0.5) \cdot \left(e^{-\psi t} - 1\right). \quad (34)$$

Here, time is defined as a change function of repetition (It) and maximum number of iterations (Max_It), and ψ has a value in the range [0, 1]:

$$t = \left(1 - \frac{\text{It}}{\text{Max\_It}}\right)^{\left(\alpha_2(\text{It}/\text{Max\_It})\right)}. \quad (35)$$

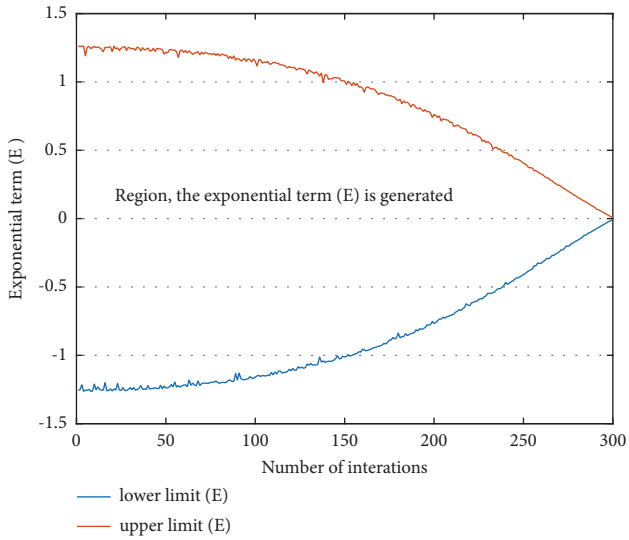

Figure 7: Exponential range (E).

α_1, α_2 are the two parameters that manage the exploration and exploitation capabilities of the algorithm.

4.1.4. Generation Rate P. As one of the most important terms in the proposed algorithm to provide the correct solution by improving the exploitation phase,

$$P = P_0 E, \tag{36}$$

where P_0 is the initial value defined as follows:

$$P_0 = P_M\left(X_{\text{eq}} - \psi X\right), \tag{37}$$

$$P_M = \begin{cases} 0.5r_1, & r_2 \geq EP, \\ 0, & r_2 \leq EP, \end{cases} \tag{38}$$

in which, r_1, r_2 are random values in the range [0, 1] and EP is a parameter that adjusts the exploration or exploitation ability of the algorithm $EP = [0,1]$. $EP = 1$, the algorithm only implements the exploration phase, leading to the difficulty of finding a globally optimal solution. When $EP = 0$, the algorithm implements the exploitation phase, which easily leads to a local optimal search. Therefore, to balance exploration and exploitation, the EP value is chosen to be 0.5.

Finally, updating the concentration in the algorithm (EO) will be as follows:

$$X^{k+1} = X_{eq} + \left(X^k - X_{eq}\right)E + \frac{P}{\psi G}\left(1 - E\right). \tag{39}$$

X_{eq} is the random choice in equilibrium pool and G is considered as unit index, which is normally set to 1.

4.2. Improved Equilibrium Optimizer Algorithm (IEO). The exploration and exploitation in the optimal algorithm greatly impact the solution result. The unbalance between the exploration and exploitation strategy of the algorithm easily leads to fast convergence (nonoptimal solution quality), or slow convergence, and it takes a long time to find a good solution. Therefore, the balance between exploration and exploitation during the optimal search of each algorithm is extremely important. In the EO algorithm, the exponential term E is defined as balance between exploration and exploitation.

However, this balance is not uniform throughout the optimization process. The way to generate the exponential term (E) from formulas (34) and (35) shows that the term (E) is dominated by the number of iterations. The relationship between the value of (E) and the number of iterations is shown in Figure 7. The size of the received limit region of E gradually decreases to zero as it approaches Max_It. This means that the algorithm's exploration will decrease according to the number of iterations. So, the result gets stuck at the local optimal solution. Although the coefficient (ψ) in equation (39) plays a role in helping (EO) to induce the mutation, the probability of mutation is very low since the coefficient ψ must be relatively small. Therefore, to strike a balance between the exploration and exploitation capabilities of the EO, this paper is proposed two adjustments for creating the new solution. First, replace the exponential term (E) in EO with the random value given by equation (40). The periodicity of the sine function allows the creation of a solution around the previous solution. This helps exploit the space between the two solutions. In addition, when the component of 3/2.rand.sign (rand-0.5) has a value >1, it helps the algorithm to explore the space outside two solutions:

$$\mathbf{E} = 3/2 \cdot \mathbf{rand} \cdot \mathbf{sign}\left(\mathbf{rand} - 0.5\right)\mathbf{sin}\left(\mathbf{rand}\right). \tag{40}$$

Furthermore, to increase the exploitation ability around the best solution of IEO, equation (41) is proposed to generate solutions that locate near the best equilibrium solution. The probability of a solution that is generated by this technique or the technique described from equations (34) to (38) is the same:

$$X^{k+1} = X^k_{eq1} + \text{rand} \cdot \left(\text{rand}\, p_1\left(X^k_{\text{pool}}\right) - \text{rand}\, p_2\left(X^k_{\text{pool}}\right)\right), \tag{41}$$

where rand is a vector of size [1 dim] containing random values distributed over the interval [0, 1], and rand $p_1\left(X^k_{\text{pool}}\right)$ and rand $p_2\left(X^k_{\text{pool}}\right)$ are random individuals in the equilibrium pool population of k^{th} loop.

The implementation of the proposed IEO algorithm to solve the OPF problem can be summarized as follows.

To apply the algorithm (IEO) to the OPF problem, each candidate is a vector consisting of control variables such as the scheduled power of the generators (excluding the slack generator) and the voltage at generator buses:

$$X_{i,j} = \left[P_{G2}, \ldots, P_{GN_G}, V_{G1}, \ldots, V_{GN_G}\right], \quad i = 1, \ldots, N_{\text{pop}} \text{ and } j = 1, \ldots, D. \tag{42}$$

Initially, each candidate is randomly generated in the upper and lower values as expression (31). The upper and lower values in expression (31) are taken from expressions (14) and (16).

Step 1. Determine the system data including branch and bus data as well as the limits of buses voltage, branches power, and generators power.

Step 2. Set the parameters for the algorithm IEO including population size N_{pop}, maximum number of iterations Max-It, and number of simulation samples Monte-Carlo.

Step 3. Calculate $N_{Montecarlo}$ sample Monte-Carlo, for wind speed and solar radiation according to Weibull and Log-normal distributions respectively. Then, using equations (25) and (28), calculate the power sample set P_{Wind} and P_{Solar}, respectively.

Step 4. Randomly initialize the Npop initial candidates using equation (29). With the control variable found in equation (42).

Step 5. Set up four equilibrium candidates and assume each candidate's target is extremely large.

Step 6. Use the Matpower toolbox to run the power flow for each candidate, and evaluate the corresponding objective function for each candidate as in equation (8), (11), or (12). In this study, the penalty coefficient method is used for inequality constraints to reject unfeasible solutions. The new objective function will be redefined through the objective functions combined with the penalty function given by (43). The penalty function for all state variables in the OPF problem is as follows:

$$F_{obj} = F\left(FC, FE, P_{\text{loss}}\right) + \text{Penalty}, \tag{43}$$

$$\begin{aligned}\text{Penalty} = {} & \lambda_{P_{sl}}\left(P_{sl} - P_{sl}^{\lim}\right)^2 + \lambda_Q \sum_{i=1}^{N_G}\left(Q_{Gi} - Q_{Gi}^{\lim}\right)^2 \\ & + \lambda_V \sum_{j=1}^{N_L}\left(V_{Lj} - V_{Lj}^{\lim}\right)^2 + \lambda_L \sum_{l=1}^{N_{\text{Line}}}\left(S_l - S_l^{\lim}\right)^2,\end{aligned} \tag{44}$$

where $\lambda_{P_{sl}}$, λ_Q, λ_V, λ_L are the penalty coefficients for the real power at the slack busP_{sl}, reactive power at all generator buses Q_{Gi}, voltage magnitude at all load bus V_{Lj}, and apparent power transmitted on branchesS_l, respectively.$P_{sl}^{\lim}$, $Q_{Gi}^{\lim}$, $V_{Lj}^{\lim}$, $S_l^{\lim}$ are the limits of the above variables, respectively.

Step 7. Update candidates in the balance group using equations (32) and (33)

Step 8. Update the respective candidate for the best solution $X_{Best} = X\text{eq1}$.

Step 9. Update the new candidates as follows:

$$X^{k+1} = \begin{cases} \text{using to Eq. (36)from Eq. (40)}, & \text{if rand} < 0.5, \\ \text{using Eq. (41)}, & \text{otherwise.} \end{cases} \tag{45}$$

Step 10. Update the candidate limit according to

$$X_i^{k+1} \begin{cases} X_{\min,i}, & \text{if } X_i^{k+1} < X_{\min,i}, \\ X_{\max,i}, & \text{if } X_i^{k+1} > X_{\max,i}, \\ X_i^{k+1}, & \text{otherwise.} \end{cases} \quad i = 1, \ldots, D. \tag{46}$$

Step 11. The new candidate will be kept to replace the old candidate, if the objective function value is better, otherwise, it will be discarded.

Step 12. Repeat Steps from 6 to 11 until the Stopping Condition Is Satisfied

Step 13. The candidate with the smallest objective function value is considered the optimal solution.

5. Simulation Results

The proposed IEO algorithm is tested on the IEEE 30-bus and IEEE 118-bus systems [49, 50]. The simulation results are done using MATLAB software and performed on a computer with Intel Core i5 CPU @ 2.7 GHz and 4 GB RAM. The study cases and control parameters of algorithms are described in Table 1, 2, respectively.

5.1. The Modified IEEE-30 Bus Test System. The data of the modified IEEE 30-bus system are summarized in Table 3. The modified IEEE 30-bus system with RES is shown as Figure 8. The thermal power plants at bus 5, bus 11, and bus 13 are replaced by two wind farms and a solar power plant, respectively. The data of wind farms and solar power plant are given in Table 4 [41]. In addition, the cost factors of RESs for direct costs, penalty costs, and reserve costs are shown as Table 5. The cost and emission coefficients of thermal generators for the IEEE 30-bus system are reported in Table 6. The simulation results of the proposed IEO method are compared to AEO, ABC, CSA, TLBO, and EO methods and the exiting other methods with three objective functions including generator cost, total emission, and power loss. To compare and evaluate methods, the study is based on criteria as follows:

(1) Compared the minimum value obtained from the methods with aims of evaluating the quality of the best solutions. To clearly compare, an improvement index (*IF*) of percentage is used:

$$\text{IF}(\%)_{\text{method}} = \frac{\text{min .of another method} - \text{minof IEO}}{\text{min .of another method}}.100\%, \tag{47}$$

Table 1: The description of study cases.

Section	Implemented method	Test system	Objective function
5.1	EO, AEO, ABC, CSA, TLBO, proposed IEO method	IEEE 30-bus system	Minimize with RES (1) generation cost (2) total emission (3) power loss
5.2	EO, AEO, ABC, CSA, TLBO, proposed IEO method	IEEE 118-bus system	Minimize generation cost (1) without RES (2) with RES

Table 2: The control parameters of the algorithms for the study cases.

Methods	Control parameters value	
	Value	Description
AEO	—	—
ABC	FoodNumber = Np/2	Number of food sources
TLBO	TF selected randomly between 1 and 2	—
CSA	Pa = 0.25	Mutation probability
EO	$a1 = 2$, $a2 = 1$ GP = 0.5	—
IEO	GP = 0.5	Mutation probability
Common parameters	Population size = 30 for all cases of IEEE 30-bus system. Population size = 50 for all cases of IEEE 118-bus system. Maximum number of iterations = 300 for all cases of IEEE 30-bus system. Maximum number of iterations = 1000 for all cases IEEE 118-bus system.	

Table 3: Summary of the modified IEEE 30-bus system.

Terms	Quantity	Details
Buses	30	[3, 49, 50]
Branches	41	[3, 49, 50]
Shunts	2	At bus 5 and bus 24
Transformers	4	At branch (6–9, 6–10, 4–12, 27–28)
Thermal generators	3	Buses: 1 (slack), 2, and 8
Wind generators	2	Buses: 5 and 11
Solar PV unit	1	Bus: 13
Control variables	11	Scheduled real power for 5 generators excluding the one at the slack bus. Bus voltage of all generator buses (6 nos.)
Connected load		$283.4 + j126.2$ (MVA)
Generator bus voltage limits	6	[0.95–1.1] p.u.
Load bus voltage limits	24	[0.95–1.05] p.u.

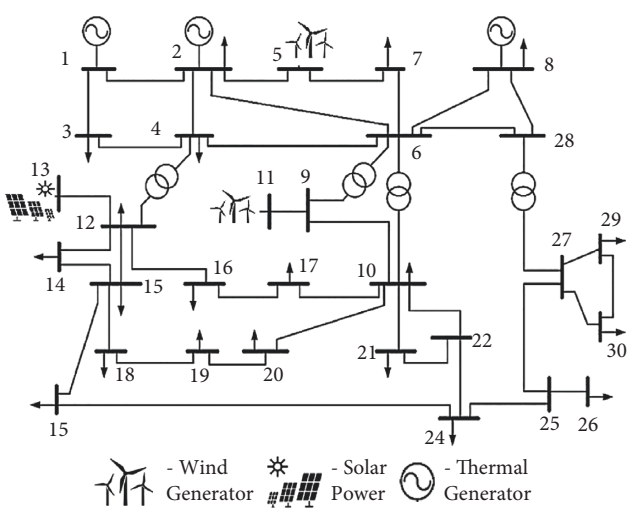

Figure 8: Modified IEEE 30-bus system with RES.

where the *IF* index has a (+) sign which means that the proposed method is better than other methods. Opposite, the *IF* index has a (−) sign which means that the proposed method is not better than other methods.

(2) Compared the standard deviation value with aims of evaluating the stability of the methods

(3) Compared the simulation time. The simulation of methods depends on the two factors: the first, the level of complexity in the way of creating new solutions of methods. Each method has its own way to generate a new solution, so the calculation time is also different. With this factor, there has not been a specific study that offers a suitable comparative solution. The second, comparing the total number of solutions generated after the method meets the stopping criterion. The total number of solutions generated depends on the number of populations

Table 4: PDF parameters of wind and solar power plants for the IEEE 30-bus system.

Wind power generating plants					Solar PV plant		
Wind farm	No. of turbines	Rated power, P_{wr} (MW)	Weibull PDF parameters	Weibull mean	Rated power, P_{sr} (MW)	Lognormal PDF parameters	Lognormal mean
1-(bus 5)	25	75	$C=9,\ k=2$	$\overline{v}=7.976$ m/s	50-(bus 13)	$\mu=6,\ \sigma=0.6$	$\overline{H}=483\,(W/m^2)$
2-(bus11)	20	60	$C=10,\ k=2$	$\overline{v}=8.862$ m/s			

Table 5: Energy source cost factor (RES) for the IEEE 30-bus system.

Cost factor for RES	Wind power generating plants		Solar PV plant
	(bus 5)	(bus 11)	(bus 13)
Direct cost factor	1.6	1.75	1.6
Penalty cost factor	1.5	1.5	1.5
Reserve cost factor	3	3	3

Table 6: Cost and emission coefficients of thermal generators for the IEEE 30-bus system.

Generator	bus	a	b	c	d	e	α	β	γ	ξ	λ
TG1	1	0	2	0.00375	18	0.037	4.091	−5.554	6.49	0.0002	6.667
TG2	2	0	1.75	0.0175	16	0.038	2.543	−6.047	5.638	0.0005	3.333
TG3	8	0	3.25	0.00834	12	0.045	5.326	−3.55	3.38	0.002	2

Table 7: The control parameters and optimal value obtained of the proposed IEO algorithm and other methods for the IEEE 30-bus system with case 1.

Control parameters	Limits		Case 1					
	Min	Max	AEO	CSA	TLBO	ABC	EO	Proposed IEO
P1 (MW)	50	200	134.9051	134.9148	134.9086	134.9079	134.9079	134.9079
P2 (MW)	20	80	28.5464	27.7752	27.6340	27.3108	27.3404	27.8087
P5 (MW)	15	50	43.7470	44.2036	44.2176	44.4118	44.5123	44.0873
P8 (MW)	10	35	10.0034	10.0294	10.0041	10.0000	10.0000	10.0000
P11 (MW)	10	30	36.2741	36.6828	36.4583	36.7607	36.4178	36.2702
P13 (MW)	12	40	35.9285	35.8012	36.1450	35.9642	36.1761	36.3030
V1 (p.u.)	0.95	1.1	1.0630	1.0817	1.0647	1.0704	1.0622	1.0766
V2 (p.u.)	0.95	1.1	1.0462	1.0636	1.0469	1.0533	1.0457	1.0592
V5 (p.u.)	0.95	1.1	1.0206	1.0395	1.0220	1.0287	1.0223	1.0338
V8 (p.u.)	0.95	1.1	1.0216	1.0283	1.0216	1.0262	1.0215	1.0299
V11(p.u.)	0.95	1.1	1.0998	1.0850	1.1000	1.0943	1.0999	1.0887
V13(p.u.)	0.95	1.1	1.0549	1.0421	1.0532	1.0497	1.0553	1.0494
Fuel cost	—	—	440.7292	438.3081	437.7190	436.6351	436.7325	438.2770
Wind cost	—	—	243.3587	246.3213	245.6025	247.3081	246.4845	44.5129
Solar cost	—	—	97.9940	97.5707	98.7158	98.1128	98.8197	99.2444
Total cost ($/$h$)	—	—	**782.082**	**782.2001**	**782.0373**	**782.0560**	**782.0367**	**782.0343**
Total emissions			0.1601	0.1603	0.1604	0.1604	0.1604	0.1603
PLoss (MW)	—	—	6.0044	6.0070	5.9677	5.9554	5.9545	5.9771

and the maximum number of iterations. A study in the literature [51] has shown that number of higher population and iterations can significantly improve quality solution, but simulation time will be longer. Especially, for the OPF problem, each new solution is performed by solving the power flow problem through iterative methods. This increases the simulation time when the number of solutions is more. In general, the total number of solutions of the methods is calculated according to one of the following three formulations:

$$\text{TNFs} = N_{\text{pop}} * (\text{Max} - \text{It}), \tag{48}$$

$$\text{TNFs} = 2 * N_{\text{pop}} * (\text{Max} - \text{It}), \tag{49}$$

$$\text{TNFs} = \left(N_{\text{pop}} + N_b\right) * (\text{Max} - \text{It}), \tag{50}$$

Table 8: The obtained results of the proposed IEO method and other exiting methods for the IEEE 30-bus system after 50 runs with case 1.

Method	Min	Average	Max	SD	N_{pop}	Max-it	TNFs	CPU times (s)	IF (%)
SHADE-SF [41]	782.503	—	—	—	—	—	24000	—	+0.059897
JS [42]	781.6387	—	—	—	100	1000	100000	—	**−0.0506116**
GWO [43]	781.40	—	—	—	30	1000	30000	429	**−0.0811748**
CSA [43]	784.77	—	—	—	30	1000	30000	668	+0.348599
ABC [43]	783.81	—	—	—	30	1000	30000	704	+0.226547
FPA [44]	777.3298	—	—	—	30	5000	150000	—	**−0.6052129**
GWO [45]	780.995	—	—	—	30	500	15000	—	**−0.1330738**
MFO [46]	780.485	—	—	—	40	500	20000	—	**−0.1985048**
AEO	782.082	782.3551	782.8942	0.1982	30	300	18000	53.01	+6.099E-03
CSA	782.2001	782.5745	783.0720	0.1943	30	300	18000	47.18	+0.021196
TLBO	782.0373	782.3001	785.1228	0.5949	30	300	18000	52.95	+3.8361E-04
ABC	782.0560	782.3940	784.8091	0.5875	30	300	18000	44.48	+2.7747E-03
EO	782.0367	782.7271	789.3457	1.4318	30	300	9000	17.21	+3.0689E-04
Proposed IEO	782.0343	782.0918	782.2878	0.0396	30	300	9000	14.73	0

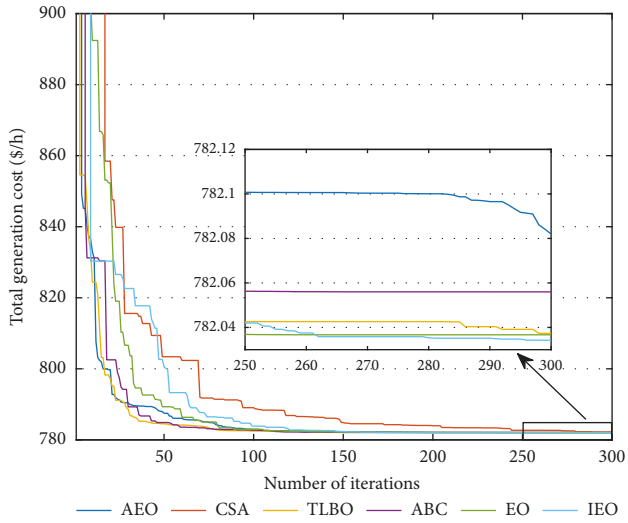

Figure 9: Convergence characteristic of the proposed IEO and other exiting methods in case 1.

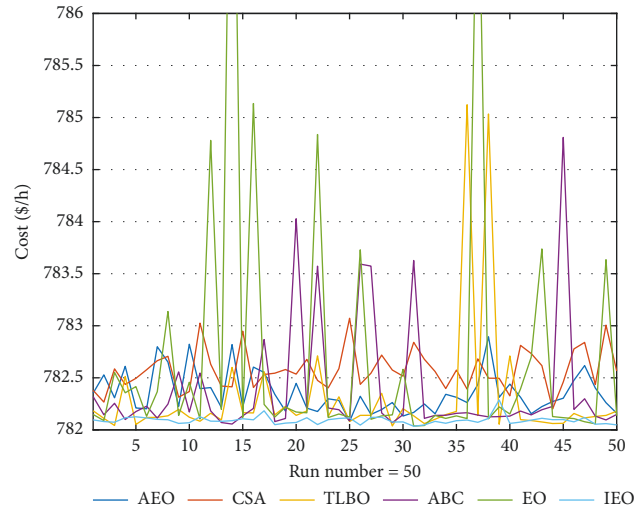

Figure 10: The generator cost after 50 runs of IEO and other methods for IEEE 30-bus systems.

where formulation (48) is applied to calculate *TNFs* for methods that generate a new solution in each iteration such as EO or IEO. Equation (49) is applied to methods that generate 2 new solutions in each iteration such as CSA, AEO, TLBO, or ABC. Formulation (50) applies to methods with probability of creating 2nd solution in each iteration such as ISSO. N_b is the number of second solutions generated in each iteration, and it is not a fixed value in each iteration. The methods, which calculate *TNFs* according to formulation (50), will normally calculate the average value of N_b in the total number of runs, from which the *TNFs* value will be calculated.

Case1. Generation cost minimization

In this case, the fuel cost for the thermal power generators is minimized based on formula (10). Table 7 presents the control parameters and optimal value obtained using the AEO, CSA, TLBO, ABC, and EO algorithm and the proposed IEO method with objective of fuel cost. Table 8 provides the best, worst, average, and standard deviation results of the AEO, CSA, TLBO, ABC, and EO and the proposed IEO method after 50 independent runs. It can be noted that from Table 8, the total fuel cost minimization of methods SHADE-SF [41], JS [42], GWO [43], FPA [44], GWO [45], and MFO [46] give better results than the IEO method in terms of the best result. However, the voltage at the load buses is violated voltage limit. The voltage limit at the load buses of these methods is considered in [0.95 p.u.–1.1 p.u.], while the voltage limit at the load buses of the proposed IEO method is [0.95 p.u.–1.05 p.u.]. Furthermore, to obtain the best value, these methods are used the number of solutions lager than the number of solutions of the proposed IEO method from 1,667 to 16,667 times, equivalent to 15000 solutions for GWO [45] and 150000 solutions for SHADE-SF [41] and FPA [44]. The five remaining methods, which are listed in Table 8, have the same system data. It is a necessary condition for the evaluation of solutions to be fair. The result in Table 8 shows that the total fuel cost is achieved 782.0343 ($/h) using the IEO algorithm, which are better than EO (782.0367 $/h), AEO (782,082 $/h),

Table 9: The obtained results of the proposed IEO method and other exiting methods for the IEEE 30-bus system after 50 runs with case 2.

Method	Min	Average	Max	SD	TNFs	CPU times (s)	IF (%)
AEO	0.091059953	0.091061197	0.091084359	$8.42e-02$	18000	54.61	$+9.598e-9$
CSA	0.091060033	0.091061869	0.091066950	$1.93e-06$	18000	45.58	$+8.684e-5$
TLBO	0.091059966	0.091060119	0.091061027	$1.79e-07$	18000	54.65	$+1.396e-5$
ABC	0.091063397	0.091236106	0.091824601	$1.65e-04$	18000	46.61	$+3.782e-3$
EO	0.091059953	0.091399058	0.099533732	$1.68e-03$	9000	16.64	$+7.964e-9$
Proposed IEO	0.091059953	0.091060288	0.091062167	$5.38e-07$	9000	13.28	0

Table 10: The control parameters and optimal values obtained from the algorithms for the IEEE 30-bus system with case 2.

Control parameters	Limits		Case 2					
	Min	Max	AEO	CSA	TLBO	ABC	EO	IEO
P1 (MW)	50	200	50.0000	50.0007	50.0001	50.0270	50.0000	50.0000
P2 (MW)	20	80	46.6298	46.6219	46.6227	46.4385	46.7613	46.6378
P5 (MW)	15	50	58.6991	71.2959	74.9598	46.9926	52.1059	64.9722
P8 (MW)	10	35	35.0000	35.0000	35.0000	35.0000	35.0000	35.0000
P11 (MW)	10	30	58.7034	42.0089	60.0000	58.2529	53.7063	56.0415
P13 (MW)	12	40	38.0266	42.4524	20.3004	50.0000	49.9796	35.5051
V1 (p.u.)	0.95	1.1	1.0554	1.0745	1.0548	1.0615	1.0754	1.0989
V2 (p.u.)	0.95	1.1	1.0411	1.0596	1.0304	1.0459	1.0364	1.0554
V5 (p.u.)	0.95	1.1	1.0093	1.0364	0.9834	1.0186	0.9978	1.0266
V8 (p.u.)	0.95	1.1	0.9900	1.0039	0.9825	1.0152	1.0034	0.9982
V11 (p.u.)	0.95	1.1	1.0285	0.9500	1.0546	1.0926	1.0609	1.0095
V13 (p.u.)	0.95	1.1	1.0785	1.0752	1.0446	1.0582	1.0098	1.0403
Fuel cost	—	—	377.3874	377.3601	377.3616	376.7612	377.8749	377.4170
Wind cost	—	—	388.7138	373.3715	463.5692	341.7264	341.0717	403.1322
Solar cost	—	—	105.1171	120.9926	57.6198	150.2402	150.1583	96.5911
Total cost ($/h)	—	—	871.2182	871.7242	898.5506	868.7278	869.1050	877.1403
Total emissions			**0.09105995**	**0.09106003**	**0.09105996**	**0.09106339**	**0.09105995**	**0.09105995**
PLoss (MW)	—	—	3.6589	3.9798	3.4830	3.3110	4.1532	4.7565

CSA (782.2001 $/h), TLBO (782.0373 $/h), and ABC (782.0560 $/h) methods. IF (%) of all methods are (+) sign. It indicates that the proposed IEO method has better improvement in the quality of the optimal solution with shorter time from 2 to 2.67 times compared to EO, AEO, CSA, TLBO, and ABC methods. In addition, the evaluation of the stability level of the methods is also carried out. The results of the fuel cost target with the minimum value obtained in 50 runs using IEO and other methods are also given in Table 8 and Figure 9. From Figure 9 and the standard deviation values in Table 8, the IEO has higher stability than other methods. The standard deviation value of the IEO (0.0396) is lower than EO (1.4318), AEO (0.1982), CSA (0.1943), TLBO (0.5949), and ABC (0.5875). The convergence speed of the IEO and other methods is shown in Figure 10. As observed, the convergence speed curve of IEO and EO shows that the EO converges earlier than the IEO. However, the EO tends to fall into the local optimum. It can be seen in Figure 10 that from the 250th iteration to the end of the iteration, the EO could not generate a better new solution. Meanwhile, the proposed IEO method still creates many new and better solutions from the 250th iteration to the end of the iteration. In addition, it is noted that using formula (31) in this study to calculate the indirect penalty cost and the reserve cost of the RES greatly reduces the optimal calculation time. As observed from Table 8, the run time of the proposed IEO method is 14.73 s which is smaller than the AEO (53.01 s), CSA (47.18 s), TLBO (52.95 s), ABC (44.48 s), and EO (17.21 s) methods.

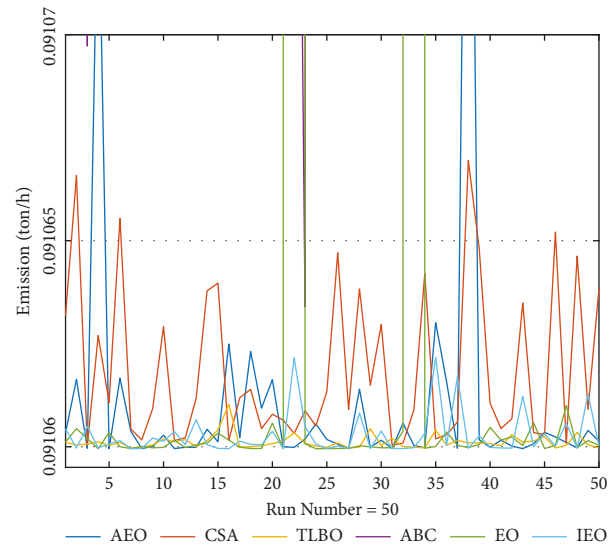

Figure 11: The emission after 50 runs of IEO and other methods for the IEEE 30-bus system.

Table 11: The control parameters and optimal values obtained from the IEO and other methods for the IEEE 30-bus system with case 3.

Control parameters	Limits		Case 3					
	Min	Max	AEO	CSA	TLBO	ABC	EO	IEO
P1 (MW)	50	200	50.0000	51.2286	50.0000	50.2162	50.0000	50.0010
P2 (MW)	20	80	29.4940	23.7634	26.5574	26.7452	25.8421	26.3951
P5 (MW)	15	50	74.9430	74.8910	74.9998	75.0000	74.9969	75.0000
P8 (MW)	10	35	34.8609	35.0000	34.9995	35.0000	34.9894	35.0000
P11 (MW)	10	30	57.0431	58.5492	57.9401	60.0000	58.2962	57.9242
P13 (MW)	12	40	39.2941	42.2208	41.1246	38.7373	41.4995	41.3009
V1 (p.u.)	0.95	1.1	1.0407	1.0471	1.0435	1.0349	1.0459	1.0430
V2 (p.u.)	0.95	1.1	1.0350	1.0392	1.0370	1.0288	1.0393	1.0366
V5 (p.u.)	0.95	1.1	1.0236	1.0293	1.0257	1.0158	1.0269	1.0256
V8 (p.u.)	0.95	1.1	1.0241	1.0265	1.0259	1.0156	1.0272	1.0257
V11 (p.u.)	0.95	1.1	1.1000	1.0963	1.0999	1.0766	1.0983	1.1000
V13 (p.u.)	0.95	1.1	1.0592	1.0561	1.0574	1.0538	1.0561	1.0579
Fuel cost	—	—	316.0890	301.6589	306.9304	308.2045	304.5591	306.4052
Wind cost	—	—	450.4822	456.8491	454.6500	463.7457	456.2010	454.5809
Solar cost	—	—	109.5512	120.1371	116.1236	107.5912	117.4901	116.7652
Total cost ($/h)	—	—	876.1223	878.6450	877.7040	879.5414	878.2502	877.7513
Total emissions			0.0930	0.0947	0.0938	0.0937	0.0940	0.0938
PLoss (MW)	—	—	**2.2352**	**2.2530**	**2.2214**	**2.2986**	**2.2242**	**2.2211**

Table 12: The obtained results of the proposed IEO method and other exiting methods for the IEEE 30-bus system after 50 runs with case 3.

Method	Min	Average	Max	SD	TNFs	CPU times (s)	IF (%)
AEO	2.2352	2.3088	2.4970	0.0621	18000	50.11	+0.630816
CSA	2.2530	2.2926	2.3712	0.0212	18000	42.38	+1.41589
TLBO	2.2214	2.2517	2.3072	0.0261	18000	53.89	+0.013505
ABC	2.2986	2.4852	2.8910	0.1153	18000	43.17	+3.371618
EO	2.2242	2.3179	3.0075	0.1197	9000	14.84	+0.139376
Proposed IEO	2.2211	2.2300	2.2614	0.0085	9000	12.47	0

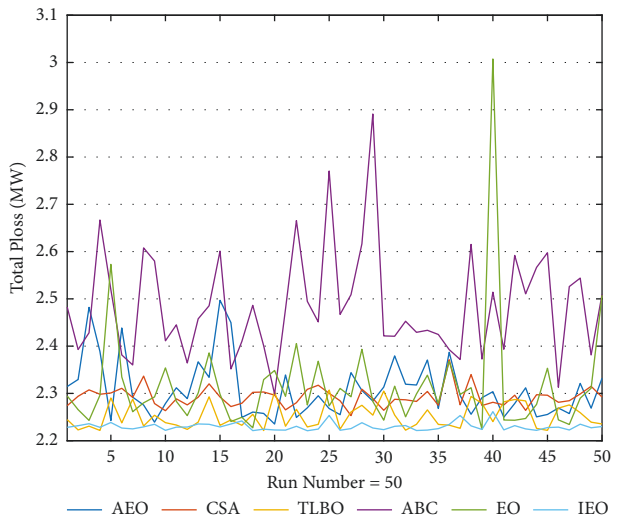

Figure 12: Power loss after 50 runs of IEO and other methods for the IEEE 30-bus system.

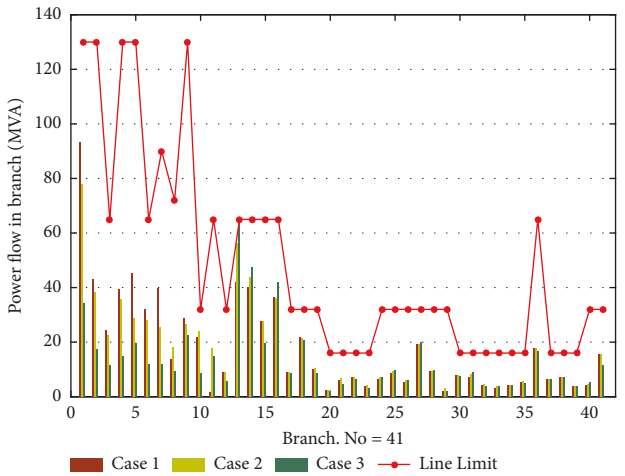

Figure 13: Power flow in branch of three cases for the IEEE 30-bus system.

Case 2. Generation emission minimization

The best, worst, and average value, and standard deviation after 50 independent runs are shown as Table 9. Table 10 presents the control parameters and optimal values of the AEO, CSA, TLBO, ABC, and EO methods and the proposed IEO method. As observed from Table 10, the AEO, TLBO, and EO algorithm, and the IEO method obtained total emission of 0.091059953 (ton/h). Meanwhile, the CSA, TLBO, and ABC algorithms have the best emissions of 0.091060033 (ton/h), 0.091059966 (ton/h), and 0.091063397 (ton/h), respectively. In general, for total emissions target,

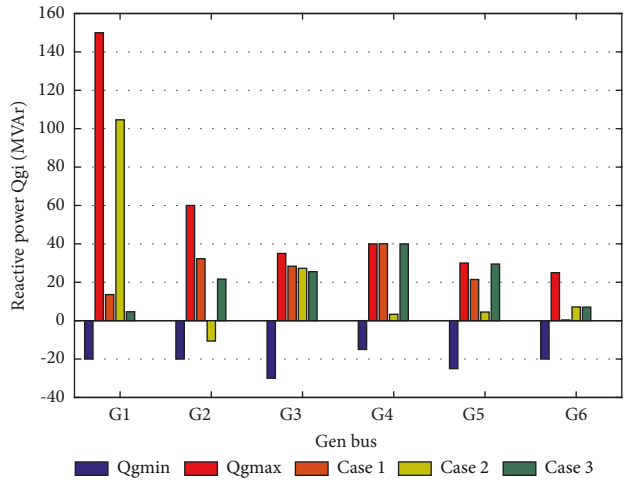

Figure 14: Reactive power of generator buses of the three cases for the IEEE 30-bus system.

Table 13: The data of the modified IEEE-118 bus system.

Terms	Quantity	Details
Buses	118	[3, 49, 50]
Branches	186	[3, 49, 50]
Shunts	14	Buses 5, 34, 37, 44, 45, 46, 48, 74, 79, 82, 83, 105 107, and 110
Transformers	11	Branches (8, 32, 36, 51, 93, 95, 102, 107, 127, 134, and 183)
Thermal generators	46	Bus: 69 (slack)
Wind generators	5	Buses: 1, 15, 27, 34, and 36
Solar PV unit	3	Buses: 54, 55, and 56
Control variables	107	Scheduled real power for 54 generators excluding the one at the slack bus. Bus voltage of all generator buses (54 nos.)
Connected load		$4242.0 + j1438.0$ (MVA)
Generator bus voltage limits	54	[0.94–1.06] p.u.
Load bus voltage limits	64	[0.94–1.06] p.u.

Table 14: PDF parameters of wind and solar power plants for the IEEE-118 bus system.

Wind power generating plants					Solar PV plant		
Wind farm	No. of turbines	Rated power, P_{wr} (in MW)	Weibull PDF parameters	Weibull mean	Rated power, P_{sr} (in MW)	Lognormal PDF parameters	Lognormal mean
1—(bus 1)	25	75			50—(bus 54)		
2—(bus 15)	25	75	$C = 9,\ k = 2$	$\overline{v} = 7.976$ m/s	50—(bus 55)	$\mu = 6,\ \sigma = 0.6$	$\overline{H} = 483\,(W/m^2)$
3—(bus 27)	25	75			50—(bus 56)		
4—(bus 34)	20	60	$C = 10,\ k = 2$	$\overline{v} = 8.862$ m/s			
5—(bus 35)	20	60					

the IEO method approximates the other methods. However, the IEO algorithm with standard deviation 5.38×10^{-7} that is more stability than other methods is shown in Table 9 and Figure 11.

Case 3. Power loss minimization

The control parameters and results of power loss obtained using the proposed IEO algorithm and other methods are shown in Table 11. The results of the solutions obtained after 50 independent runs are presented in Table 12. Figure 12 presents stability level of the IEO method compared with other algorithms after 50 independent runs. From Table 11, it can be seen that the power loss of the IEO (2.2211 MW) is lower than AEO (2.2352 MW), CSA(2.2530 MW), TLBO (2.2214 MW), ABC (2.2986 MW), and EO (2.2242 MW). Moreover, the standard deviation of IEO algorithm is better than compared to other methods as shown in Figure 12. Besides, Figure 13 and 14 present the branch power flow and reactive power of generator buses for three cases. From these figures, it can be noted that the branch power flow and reactive power of generator buses are within allowable limit.

Table 15: Energy source cost factor (RES) with the IEEE118-bus system.

Cost factor for energy source RES	Wind power generating plants					Solar PV plant		
	(bus 1)	(bus 15)	(bus 27)	(bus 34)	(bus 35)	(bus 54)	(bus 55)	(bus 56)
Direct cost factor	15	15	15	15	15	15	15	15
Penalty cost factor	20	20	20	22	22	18	20	20
Reserve cost factor	40	40	40	40	40	40	40	40

Table 16: The results obtained after 50 independent runs for the 118-bus system without RES of the proposed IEO method and other algorithms.

Method	Min	Average	Max	SD	N_{pop}	Max-It	TNFs	CPU times (s)	IF (%)
AEO	129821.5088	130675.3582	131305.6505	442.83023	50	1000	100000	541.21	+0.000604
CSA	129869.6693	131081.6882	132295.4056	690.62946	50	1000	100000	512.76	+0.037687
TLBO	129834.0084	130263.1053	130820.2169	300.04403	50	1000	100000	550.43	+0.010231
ABC	131035.1913	132761.3158	135201.9193	1216.3549	50	1000	100000	478.02	+0.926824
BBO [50]	135263.7289	135622.6172	136611.2731	335.0166	90	2500	225000	—	+4.023994
ICBO [29]	135121.570	135175.672	—	—	90	2500	225000	—	+3.923019
BSA [50]	135333.4743	135502.6493	135689.1275	93.1975	90	2500	225000	—	+4.073456
EO	129876.0705	130728.6536	136398.2541	1566.9101	50	1000	50000	168.82	+0.042614
Proposed IEO	129820.7252	130025.2172	131153.2047	245.13772	50	1000	50000	132.04	0

Table 17: The results obtained after 50 independent runs for the 118-bus system with RES of the proposed IEO method and other algorithms.

Method	Min	Average	Max	SD	N_{pop}	Max-it	TNF	CPU times (s)	IF (%)
AEO	129493.8171	138800.0481	148865.3491	6091.0705	50	1000	100000	628.13	+0.23759
CSA	129757.5576	140077.2324	148943.7147	5701.9366	50	1000	100000	579.64	+0.44036
TLBO	129409.2005	133942.2353	139174.8786	2796.3609	50	1000	100000	605.16	+0.17235
ABC	132472.8857	149873.3151	170494.0097	10438.8178	50	1000	100000	562.11	+2.48106
EO	129251.2277	138703.0949	184497.4137	14185.9052	50	1000	50000	216.47	+0.05034
IEO	129186.1520	130831.7454	139865.8795	1900.8865	50	1000	50000	178.84	0

5.2. The IEEE 118-Bus System. The IEEE 118-bus system is used to test the performance of the IEO in terms of global optimal value and stability ability for a large system. Besides, a modified IEEE 118-bus system with the participation of RES is also considered in this case. The IEEE118-bus system includes 54 thermal units, 99 load buses, 186 branches, 9 transformers, and 12 reactive power compensators [3, 49, 50]. In the modified IEEE 118-bus system, the thermal power plants are replaced by wind farms and solar power plants. The thermal power plants at buses 1, 15, 27, 34, and 36 are replaced by wind farms, while three solar power plants are replaced for thermal power plants at buses 54, 55, and 56. The data of IEEE 118 bus system and the parameters of wind farm and solar plants are given in Table 13 and 14, respectively. The direct cost coefficients, penalty costs, and storage costs of the RES are given in Table 15. In this case, the fuel cost for the thermal power generators is minimized based on formula (9).

Case 4. The IEEE 118-bus system without RES

The control parameter and fuel cost obtained from the proposed IEO algorithm for the IEEE 118-bus system without RES are presented in Table 16. Table 17 shows the best, average, and worst results after 50 independent runs, as well as the simulation time and number of new solutions to obtain the best result of the proposed IEO algorithm and other methods for case without RES. Figure 15 presents convergence characteristic of the proposed IEO method and other methods for the IEEE118-bus system without RES.

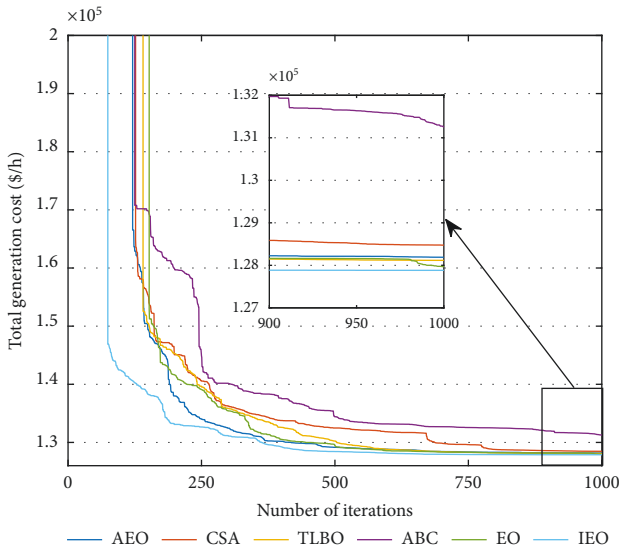

Figure 15: Convergence characteristic of the proposed IEO method and other methods for the IEEE118-bus system without RES.

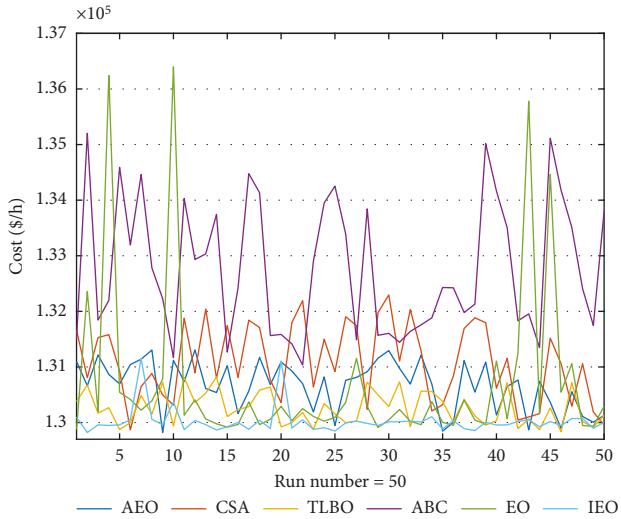

Figure 16: The generator cost after 50 runs of the proposed IEO and other methods for IEEE 118-bus systems without RES.

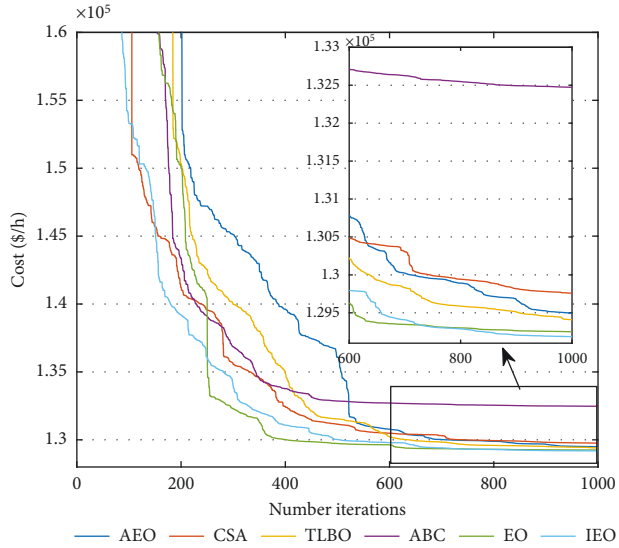

Figure 17: Convergence characteristic of the proposed IEO method and other methods for the IEEE118-bus system with RES.

Besides, the results obtained after 50 independent runs of the proposed IEO method and other methods are shown in Figure 16. From Table 17, it can be seen that the IF index of the methods is signed (+). This shows that the proposed IEO method has the best obtained value of (129820.7252) with only 50000 new solutions which is smaller than AEO, CSA, TLBO, ABC, EO, and BBO [50], ICBO [29], and BSA [50]. The standard deviation achieved from the proposed IEO (245.13772) is smaller than the original EO algorithm (1566.9101). In addition, observed average simulation time of the methods in Table 17 also shows the robustness of the IEO method compared to other methods. The proposed IEO method takes only 132.04(s) time per run while AEO (541.21 s), CSA (512.76 s) TLBO (550.43 s), ABC (478.02 s), and EO (168.82 s).

Case 5. Modified IEEE 118-bus system with RES

A modified IEEE 118 bus system with RES is used to test the proposed IEO algorithm. The control parameters and fuel cost obtained from the IEEE 118-bus system with RES using the IEO method are presented in Table 16. Figure 17 shows convergence characteristic of the proposed IEO method and other methods for the IEEE118-bus system with RES. Besides, the results obtained after 50 independent runs from the proposed IEO method and other algorithms also are given in Table 18 and Figure 18. From Table 18, it can be seen that the total fuel cost of IEO (129186.1520) is better than EO (129251.2277), AEO (129493.8171), CSA (129757.5576), TLBO (129409.2005), and ABC (132472.8857). As observed from Table 18 and Figure 17 and 18, the IEO algorithm can obtain better

Table 18: The control parameters and fuel cost obtained from the IEEE 118-bus system without RES and with RES using the proposed IEO method.

Bus no.	Control parameter	Without RES	With RES	Control parameter	Without RES	With RES
1	PG01 (MW)	29.9754	34.2786	V01 (p.u.)	0.9711	1.0007
4	PG04 (MW)	0.0002	0.0000	V04 (p.u.)	0.9993	1.0274
6	PG06 (MW)	0.0000	0.4252	V06 (p.u.)	0.9885	1.0178
8	PG08 (MW)	0.0002	0.0004	V08 (p.u.)	1.0207	1.0295
10	PG010 (MW)	400.0368	394.7797	V10 (p.u.)	1.0600	1.0600
12	PG012 (MW)	85.7587	84.5533	V12 (p.u.)	0.9848	1.0172
15	PG015 (MW)	20.2632	35.2944	V15 (p.u.)	0.9818	1.0302
18	PG018 (MW)	0.0000	0.0175	V18 (p.u.)	0.9868	1.0349
19	PG019 (MW)	27.4302	11.8650	V19 (p.u.)	0.9791	1.0289
24	PG24 (MW)	0.0000	0.0000	V24 (p.u.)	1.0235	1.0525
25	PG25 (MW)	193.5861	190.2270	V25 (p.u.)	1.0569	1.0600
26	PG26 (MW)	280.3155	275.1830	V26 (p.u.)	1.0369	1.0246
27	PG27 (MW)	11.6272	34.4155	V27 (p.u.)	1.0144	1.0451
31	PG31 (MW)	7.2303	7.1524	V31 (p.u.)	0.9995	1.0326
32	PG32 (MW)	16.4180	0.0133	V32 (p.u.)	1.0095	1.0421
34	PG34 (MW)	9.4437	29.7483	V34 (p.u.)	1.0055	1.0287
36	PG36 (MW)	10.8060	29.6131	V36 (p.u.)	1.0013	1.0231
40	PG40 (MW)	51.2751	59.9937	V40 (p.u.)	0.9945	1.0164
42	PG42 (MW)	44.0729	37.4122	V42 (p.u.)	1.0014	1.0152
46	PG46 (MW)	19.0633	18.8211	V46 (p.u.)	1.0187	1.0119
49	PG49 (MW)	192.7917	191.8848	V49 (p.u.)	1.0363	1.0265
54	PG54 (MW)	49.9969	33.7510	V54 (p.u.)	1.0192	0.9959
55	PG55 (MW)	31.8831	32.3740	V55 (p.u.)	1.0186	0.9929
56	PG56 (MW)	34.2560	32.3598	V56 (p.u.)	1.0185	0.9942
59	PG59 (MW)	149.2530	150.1249	V59 (p.u.)	1.0329	1.0114
61	PG61 (MW)	148.5864	147.0525	V61 (p.u.)	1.0308	1.0186
62	PG62 (MW)	0.0020	0.0581	V62 (p.u.)	1.0292	1.0158
65	PG65 (MW)	349.3146	348.1722	V65 (p.u.)	0.9977	0.9948
66	PG66 (MW)	348.6932	339.5984	V66 (p.u.)	1.0506	1.0381
69	PG69 (MW)	453.3021	450.1949	V69 (p.u.)	1.0447	1.0450
70	PG70 (MW)	0.0000	0.0004	V70 (p.u.)	1.0069	1.0223
72	PG72 (MW)	0.0000	0.2237	V72 (p.u.)	1.0101	1.0600
73	PG73 (MW)	0	0.0578	V73 (p.u.)	1.0065	1.0289
74	PG74 (MW)	16.6077	14.7015	V74 (p.u.)	0.9923	0.9981
76	PG76 (MW)	19.3987	17.8025	V76 (p.u.)	0.9823	0.9806
77	PG77 (MW)	0.0000	0.2165	V77 (p.u.)	1.0197	1.0115
80	PG80 (MW)	431.6642	426.6092	V80 (p.u.)	1.0342	1.0199
85	PG85 (MW)	0.0005	0.0000	V85 (p.u.)	1.0263	1.0309
87	PG87 (MW)	3.6555	3.6864	V87 (p.u.)	1.0273	1.0598
89	PG89 (MW)	500.0391	502.9658	V89 (p.u.)	1.0418	1.0458
90	PG90 (MW)	0.0046	0.0001	V90 (p.u.)	1.0183	1.0211
91	PG91 (MW)	0.0000	0.0022	V91 (p.u.)	1.0196	1.0227
92	PG92 (MW)	0.0005	0.0000	V92 (p.u.)	1.0260	1.0242
99	PG99 (MW)	0.0000	0.0181	V99 (p.u.)	1.0232	1.0044
100	PG100 (MW)	230.7860	228.6403	V100 (p.u.)	1.0258	1.0109
103	PG103 (MW)	38.2256	38.4942	V103 (p.u.)	1.0201	1.0026
104	PG104 (MW)	0.0000	0.0000	V104 (p.u.)	1.0108	0.9970
105	PG105 (MW)	4.6184	0	V105 (p.u.)	1.0092	0.9968
107	PG107 (MW)	30.3030	38.6618	V107 (p.u.)	1.0030	0.9973
110	PG110 (MW)	8.7753	8.0400	V110 (p.u.)	1.0171	0.9907
111	PG111 (MW)	35.0925	35.3071	V111 (p.u.)	1.0295	0.9939
112	PG112 (MW)	38.0497	36.1964	V112 (p.u.)	1.0109	0.9831
113	PG113 (MW)	0.1055	0.0326	V113 (p.u.)	1.0021	1.0431
116	PG116 (MW)	0.0005	0.0000	V116 (p.u.)	0.9945	0.9942
Fuel cost ($/h)	—	119790.1728				
Wind cost ($/h)	—	6163.7140				
Solar cost ($/h)	—	3232.2652				
Total cost ($/h)	**129820.7252**	**129186.1520**				

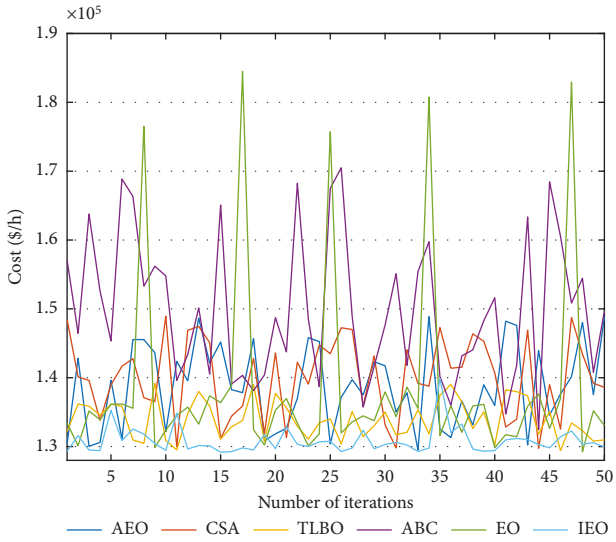

Figure 18: The generator cost after 50 runs of the proposed IEO method and other methods for the IEEE 118-bus system with RES.

values with smaller standard deviations than the EO, AEO, CSA, TLBO, and ABC methods. The simulation results demonstrate the effectiveness and robustness of the IEO method in solving the OPF problem with RES for large systems. In addition, from Table 18, it can be seen that the run time of the proposed IEO method for solving the OPF problem with RES is 178.84(s) which is smaller than EO (216.47 s), AEO (628.13 s), CSA (579.64 s), TLBO (605.16 s), and ABC (562.11 s) methods. It is confirmed that using proposed probability equation (31) for calculating the cost indirectly of RES can reduce the simulation time compared to the other approaches.

6. Conclusion

Finding the best solution for OPF problem with RES is one of challenges for many algorithms, especially in complex systems. In this paper, the IEO algorithm is proposed to deal with OPF problem with RES for three other objective functions. The suggested IEO technique is tested on IEEE 30 and IEEE 118 bus system. The obtained results of suggested approach are compared with EO, AEO, CSA, TLBO, and ABC algorithms and other exiting methods. For the IEEE 30-bus system with RES, the total fuel cost is achieved 782.0343 ($/h) using the IEO algorithm, which are better than EO (782.0367 $/h), AEO (782,082 $/h), CSA (782.2001 $/h), TLBO (782.0373 $/h), and ABC (782.0560). Besides, simulation time of the IEO is smaller from 2 to 2.67 compared to EO, AEO, CSA, TLBO, and ABC methods. In addition, the standard deviation value of the IEO (0.0396) is lower than EO (1.4318), AEO (0.1982), CSA (0.1943), TLBO (0.5949), and ABC (0.5875). For large-scale IEEE 118-bus with RES systems, using proposed probability equation (29) in the proposed IEO method decreases the run time higher compared to other methods. The simulation results show that, the proposed IEO algorithm also is one of effective and reliable methods for dealing problem of OPF with RES in large-scale and complex systems.

Nomenclature

F_C:	Total generation cost ($/h) of thermal units
$N_{TG}, N_{\text{wind}}, N_{\text{solar}}$:	Number of thermal power plants, wind power plants, and solar power plants
C_{wind}:	The cost of wind power
$N_{\text{montecarlo}}$:	Number of simulations Monte-Carlo
C_{solar}:	The cost of solar power
$P_{G,i}, Q_{G,i}$:	Power at the i^{th} generator node
FE:	Total emission
$P_{L,i}, Q_{L,i}$:	Power at the j^{th} load node
P_{loss}:	Power losses
VG, VL:	Voltage magnitude at the generator and load buses
g_j, h_k:	Direct cost coefficients of the j^{th} wind power and the k^{th} solar power plant
$P_{Gi,\,\text{min}}, Q_{Gi,\,\text{min}}$:	Minimum output power for power i^{th} plant
$K_{wL,j}, K_{sL,k}$:	Reserve cost coefficients of j^{th} wind power plant and k^{th} solar power plant
$P_{Gi,\,\text{max}}, Q_{Gi,\,\text{max}}$:	Maximum output power for power i^{th} plant
$K_{wH,j}, K_{sH,k}$:	Penalty cost coefficients of j^{th} wind power plant and k^{th} solar power plant
$V_{Gi,\,\text{min}}, V_{Gi,\,\text{max}}$:	Voltage magnitude limit at generator nodes
$P_{TG,i}, Q_{TG,i}$:	Real power and reactive power of the ith thermal power plant
$V_{Li,min}, V_{Li,max}$:	Voltage magnitude limit at load nodes
$P_{\text{s.wind},j}$:	Scheduled power of the j^{th} wind power plant
$S_l, S_{l,\,\text{max}}$:	Transmission capacity and line limit
$P_{\text{s.solar},k}$:	Scheduled power of the k^{th} solar power plant v wind speed (the wind speed random variable) (m/s)
$N_G, N_L, N_{\text{Line}}$:	Number of power plants, load nodes, and transmission lines v_{in} cut-in wind speed (m/s)
N_C, N_T:	Number of transformer tap and switchable capacitor capacity v_r rated wind speed (m/s)
δ_i, δ_j:	Voltage phase angle of node i^{th} and node j^{th} v_{out} cut-out wind speed (m/s)
$\theta_{i,j}$L:	The angle of the bus conduction matrix Y with two nodes i^{th} and j^{th}.

Data Availability

The data used to support the findings of this study are included within the article.

Conflicts of Interest

The authors declare that they have no conflicts of interest.

Acknowledgments

We acknowledge Ho Chi Minh City University of Technology (HCMUT), VNU-HCM, for the support of time and facilities for this study.

References

[1] M. Ebeed, S. Kamel, and F. Jurado, "Optimal power flow using recent optimization techniques," *Classical and Recent Aspects of Power System Optimization*, Elsevier, Amsterdam, Netherlands, 2018.

[2] R. Mota-Palomino and V. H. Quintana, "Sparse reactive power scheduling by a penalty-function linear programming technique," *IEEE Transactions on Power Systems*, vol. 1, no. 3, pp. 31–39, 1986.

[3] O. Alsac and B. Stott, "Optimal load flow with steady-state security," *IEEE Transactions on Power Apparatus and Systems*, vol. PAS-93, no. 3, pp. 745–751, 1974.

[4] D. I. Sun, B. Ashley, B. Brewer, A. Hughes, and W. F. Tinney, "Optimal power flow by Newton approach," *IEEE Transactions on Power Apparatus and Systems*, vol. PAS-103, pp. 2864–2880, 1984.

[5] R. C. Burchett, H. H. Happ, and D. R. Vierath, "Quadratically convergent optimal power flow," *IEEE Transactions on Power Apparatus and Systems*, vol. 103, pp. 3267–3275, 1984.

[6] X. Yan and V. H. Quintana, "Improving an interior-point-based OPF by dynamic adjustments of step sizes and tolerances," *IEEE Transactions on Power Systems*, vol. 14, no. 2, pp. 709–717, 1999.

[7] T. Hariharan and K. Mohana Sundaram, "Multiobjective optimal power flow using particle swarm optimization," *International Journal of Control Theory and Applications*, vol. 9, no. 2, pp. 671–679, 2016.

[8] A. Bhattacharya and P. K. Roy, "Solution of multi-objective optimal power flow using gravitational search algorithm," *IET Generation, Transmission & Distribution*, vol. 6, no. 8, p. 751, 2012.

[9] S. Duman, U. Güvenç, Y. Sönmez, and N. Yörükeren, "Optimal power flow using gravitational search algorithm," *Energy Conversion and Management*, vol. 59, pp. 86–95, 2012.

[10] A. A. Abou El Ela, M. A. Abido, and S. R. Spea, "Optimal power flow using differential evolution algorithm," *Electric Power Systems Research*, vol. 80, no. 7, pp. 878–885, 2010.

[11] H. Pulluri, R. Naresh, and V. Sharma, "Application of stud krill herd algorithm for solution of optimal power flow problems," *International Transactions on Electrical Energy Systems*, vol. 27, no. 6, Article ID e2316, 2017.

[12] M. Rezaei Adaryani and A. Karami, "Artificial bee colony algorithm for solving multi-objective optimal power flow problem," *International Journal of Electrical Power & Energy Systems*, vol. 53, no. 1, pp. 219–230, 2013.

[13] A. Bhattacharya and P. K. Chattopadhyay, "Application of biogeography-based optimisation to solve different optimal power flow problems," *IET Generation, Transmission & Distribution*, vol. 5, no. 1, p. 70, 2011.

[14] W. Warid, H. Hizam, N. Mariun, and N. I. Abdul-Wahab, "Optimal power flow using the Jaya algorithm," *Energies*, vol. 9, no. 9, p. 678, 2016.

[15] N. Sinsuphan, U. Leeton, and T. Kulworawanichpong, "Optimal power flow solution using improved harmony search method," *Applied Soft Computing*, vol. 13, no. 5, pp. 2364–2374, 2013.

[16] H. R. E. H. Bouchekara, M. A. Abido, and M. Boucherma, "Optimal power flow using teaching-learning-based optimization technique," *Electric Power Systems Research*, vol. 114, pp. 49–59, 2014.

[17] A. F. Attia, R. A. El Sehiemy, and H. M. Hasanien, "Optimal power flow solution in power systems using a novel Sine-Cosine algorithm," *International Journal of Electrical Power & Energy Systems*, vol. 99, pp. 331–343, 2018.

[18] M. Rambabu, G. V. Nagesh Kumar, and S. Sivanagaraju, "Optimal power flow of integrated renewable energy system using a thyristor controlled seriescompensator and a grey-Wolf algorithm," *Energies*, vol. 12, 2019.

[19] A. A. A. Mohamed, Y. S. Mohamed, A. A. M. El-Gaafary, and A. M. Hemeida, "Optimal power flow using moth swarm algorithm," *Electric Power Systems Research*, vol. 142, pp. 190–206, 2017.

[20] D. T. Long, T. T. Nguyen, N. A. Nguyen, and L. A. T. Nguyen, "An effective method for maximizing social welfare in electricity market via optimal TCSC installation," *Engineering, Technology & Applied Science Research*, vol. 9, no. 6, pp. 4946–4955, 2019.

[21] T. L. Duong, T. T. Nguyen, N. A. Nguyen, and T. Kang, "Available transfer capability determination for the electricity market using cuckoo search algorithm," *Engineering, Technology & Applied Science Research*, vol. 10, no. 1, pp. 5340–5345, 2020.

[22] T. Niknam, M. R. Narimani, and R. Azizipanah-Abarghooee, "A new hybrid algorithm for optimal power flow considering prohibited zones and valve point effect," *Energy Conversion and Management*, vol. 58, pp. 197–206, 2012.

[23] J. Radosavljević, D. Klimenta, M. Jevtić, and N. Arsić, "Optimal power flow using a hybrid optimization algorithm of particle swarm optimization and gravitational search algorithm," *Electric Power Components and Systems*, vol. 43, no. 17, pp. 1958–1970, 2015.

[24] T. L. Duong, N. A. Nguyen, and T. T. Nguyen, "A newly hybrid method based on cuckoo search and sunflower optimization for optimal power flow problem," *Sustainability*, vol. 12, no. 13, p. 5283, 2020.

[25] M. Abdo, S. Kamel, M. Ebeed, J. Yu, and F. Jurado, "Solving non-smooth optimal power flow problems using a developed grey wolf optimizer," *Energies*, vol. 11, no. 7, p. 1692, 2018.

[26] T. Niknam, M. R. Narimani, J. Aghaei, S. Tabatabaei, and M. Nayeripour, "Modified honey bee mating optimisation to solve dynamic optimal power flow considering generator constraints," *IET Generation, Transmission & Distribution*, vol. 5, no. 10, p. 989, 2011.

[27] T. Niknam, M. R. Narimani, M. Jabbari, and A. R. Malekpour, "A modified shuffle frog leaping algorithm for multi-objective optimal power flow," *Energy*, vol. 36, no. 11, pp. 6420–6432, 2011.

[28] M. A. Taher, S. Kamel, F. Jurado, and M. Ebeed, "An improved moth-flame optimization algorithm for solving optimal power flow problem," *International Transactions on Electrical Energy Systems*, vol. 29, no. 3, Article ID e2743, 2018.

[29] H. R. E. H. Bouchekara, A. E. Chaib, M. A. Abido, and R. A. El-Sehiemy, "Optimal power flow using an improved colliding bodies optimization algorithm," *Applied Soft Computing*, vol. 42, pp. 119–131, 2016.

[30] M. Ghasemi, S. Ghavidel, M. M. Ghanbarian, M. Gharibzadeh, and A. Azizi Vahed, "Multi-objective optimal power flow considering the cost, emission, voltage deviation and power losses using multi-objective modified

imperialist competitive algorithm," *Energy*, vol. 78, pp. 276–289, 2014.

[31] M. Rizwan, L. Hong, W. Muhammad, S. W. Azeem, and Y. Li, "Hybrid Harris Hawks optimizer for integration of renewable energy sources considering stochastic behavior of energy sources," *International Transactions on Electrical Energy Systems*, vol. 31, no. 2, 2021.

[32] S. Duman, S. Rivera, J. Li, and L. Wu, "Optimal power flow of power systems with controllable wind-photovoltaic energy systems via differential evolutionary particle swarm optimization," *International Transactions on Electrical Energy Systems*, vol. 30, no. 4, 2019.

[33] M. H. Sulaiman, Z. Mustaffa, A. J. Mohamad, M. M. Saari, and M. R. Mohamed, "Optimal power flow with stochastic solar power using barnacles mating optimizer," *International Transactions on Electrical Energy Systems*, vol. 31, no. 5, 2021.

[34] C. Shilaja and T. Arunprasath, "Optimal power flow using moth swarm algorithm with gravitational search algorithm considering wind power," *Future Generation Computer Systems*, vol. 98, pp. 708–715, 2019.

[35] C. S. Saunders, "Point estimate method addressing correlated wind power for probabilistic optimal power flow," *IEEE Transactions on Power Systems*, vol. 29, no. 3, pp. 1045–1054, 2014.

[36] T. Mahmoud, Z. Y. Dong, and J. Ma, "An advanced approach for optimal wind power generation prediction intervals by using self-adaptive evolutionary extreme learning machine," *Renewable Energy*, vol. 126, pp. 254–269, 2018.

[37] M. Aien, M. Fotuhi-Firuzabad, and M. Rashidinejad, "Probabilistic optimal power flow in correlated hybrid wind–photovoltaic power systems," *IEEE Transactions on Smart Grid*, vol. 5, no. 1, pp. 130–138, 2014.

[38] L. Shi, C. Wang, L. Yao, Y. Ni, and M. Bazargan, "Optimal power flow solution incorporating wind power," *IEEE Systems Journal*, vol. 6, no. 2, pp. 233–241, 2012.

[39] M. A. M. Shaheen, H. M. Hasanien, and A. Al-Durra, "Solving of optimal power flow problem including renewable energy resources using HEAP optimization algorithm," *IEEE Access*, vol. 9, pp. 35846–35863, 2021.

[40] Z. M. Ali, S. H. E. A. Aleem, I. Ahmed, and B. S. Mahmoud, "Economical-environmental-technical operation of power networks with high penetration of renewable energy systems using multi-objective coronavirus herd immunity algorithm," *Mathematics*, vol. 10, no. 7, p. 1201, 2022.

[41] P. P. Biswas, P. N. Suganthan, and G. A. J. Amaratunga, "Optimal power flow solutions incorporating stochastic wind and solar power," *Energy Conversion and Management*, vol. 148, pp. 1194–1207, 2017.

[42] M. Farhat, S. Kamel, A. M. Atallah, and B. Khan, "Optimal power flow solution based on jellyfish search optimization considering uncertainty of renewable energy sources," *IEEE Access*, vol. 9, pp. 100911–100933, 2021.

[43] I. U. Khan, N. Javaid, K. A. A. Gamage, C. J. Taylor, S. Baig, and X. Ma, "Heuristic algorithm based optimal power flow model incorporating stochastic renewable energy sources," *IEEE Access*, vol. 8, pp. 148622–148643, 2020.

[44] M. Abdullah, N. Javaid, I. U. Khan, Z. A. Khan, A. Chand, and N. Ahmad, "Optimal Power Flow with Uncertain Renewable Energy Sources Using Flower Pollination Algorithm," *Advances in Intelligent Systems and Computing*, Springer International Publishing, Berlin, Germany, 2020.

[45] S. B. Pandya and H. R. Jariwala, "Renewable energy resources integrated multi-objective optimal power flow using non-dominated sort grey wolf optimizer," *Journal of Green Engineering*, vol. 10, no. 1, pp. 180–205, 2020.

[46] S. B. Pandya and H. R. Jariwala, "Stochastic renewable energy resources integrated multi-objective optimal power flow," *TELKOMNIKA (Telecommunication Computing Electronics and Control)*, vol. 18, no. 3, p. 1582, 2020.

[47] A. Faramarzi, M. Heidarinejad, B. Stephens, and S. Mirjalili, "Equilibrium optimizer: a novel optimization algorithm," *Knowledge-Based Systems*, vol. 191, Article ID 105190, 2020.

[48] C. Gong, "IEC international standard 61400-1," *Order - A Journal on the Theory of Ordered Sets and its Applications*, pp. 1–9, 3rd edition, 2008.

[49] R. D. Zimmerman and C. E. Murillo-s, "Matpower manual de usuario Version 7.1," 2020, https://matpower.org/doc/.

[50] A. E. Chaib, H. R. E. H. Bouchekara, R. Mehasni, and M. A. Abido, "Optimal power flow with emission and non-smooth cost functions using backtracking search optimization algorithm," *International Journal of Electrical Power & Energy Systems*, vol. 81, pp. 64–77, 2016.

[51] M. Mernik, S. H. Liu, D. Karaboga, and M. Črepinšek, "On clarifying misconceptions when comparing variants of the Artificial Bee Colony Algorithm by offering a new implementation," *Information Sciences*, vol. 291, pp. 115–127, 2015.